University of Alberta

Reflection and Transmission Problems in Vertically Inhomogeneous Elastic Media

by

Adam Mirza Baig ©

A thesis submitted to the Faculty of Graduate Studies and Research

in partial fulfillment of the requirements for the degree

of

Master of Science

in

Geophysics

Department of Physics

Edmonton, Alberta

Fall 1999

National Library of Canada
Acquisitions and Bibliographic Services
395 Wellington Street
Ottawa ON K1A 0N4
Canada

Bibliothèque nationale du Canada
Acquisitions et services bibliographiques
395, rue Wellington
Ottawa ON K1A 0N4
Canada

Your file Votre référence

Our file Notre référence

The author has granted a non-exclusive licence allowing the National Library of Canada to reproduce, loan, distribute or sell copies of this thesis in microform, paper or electronic formats.

L'auteur a accordé une licence non exclusive permettant à la Bibliothèque nationale du Canada de reproduire, prêter, distribuer ou vendre des copies de cette thèse sous la forme de microfiche/film, de reproduction sur papier ou sur format électronique.

The author retains ownership of the copyright in this thesis. Neither the thesis nor substantial extracts from it may be printed or otherwise reproduced without the author's permission.

L'auteur conserve la propriété du droit d'auteur qui protège cette thèse. Ni la thèse ni des extraits substantiels de celle-ci ne doivent être imprimés ou autrement reproduits sans son autorisation.

0-612-47005-9

Canada

UNIVERSITY OF ALBERTA
LIBRARY RELEASE FORM

NAME OF AUTHOR:	Adam Mirza Baig
TITLE OF THESIS:	Reflection and Transmission Problems in Vertically Inhomogeneous Elastic Media
DEGREE:	Master of Science
YEAR THE DEGREE GRANTED:	1999

Permission is hereby granted to the University of Alberta Library to reproduce single copies of this thesis and to lend or sell such copies for private, scholarly, or scientific research purposes only.

The author reserves all other publication and other rights in association with the copyright in the thesis, and except as hereinbefore provided, neither the thesis nor any substantial portion thereof may be printed or otherwise reproduced in any material form whatever without the author's prior written permission.

Adam Mirza Baig
5827 181 street
Edmonton, Alta.
T6M 1V7

August 26, 1999

UNIVERSITY OF ALBERTA

FACULTY OF GRADUATE STUDIES AND RESEARCH

The undersigned certify that they have read, and recommend to the Faculty of Graduate Studies and Research for acceptance, a thesis entitled "Reflection and Transmission Problems in Vertically Inhomogeneous Elastic Media", submitted by Adam Mirza Baig in partial fulfillment of the requirements for the degree of Master of Science in Geophysics.

Professor Douglas R. Schmitt

Professor Mohsen Razavy

Assistant Professor Mauricio D. Sacchi

Assistant Professor Andrew B. G. Bush

Date: August 26, 1999

I would like to dedicate this thesis to the memories of Tariq Mirza Baig and to Dr. Frantisek Hron

Abstract

The work in this thesis is devoted to modelling two effects. The first effect we studied is that of the focussing and defocussing of seismic energy after reflection or transmission from a boundary due to seismic velocity inhomogeneity in the vicinity of the boundary. This work was done to characterize how velocity gradients would affect the amplitudes of a seismic signal and to emphasize that inhomogeneity cannot be ignored in seismology. The second effect studied is that of energy partitioning at a boundary defined by a change in seismic velocity gradient rather than that of a discrete change in material properties. We wanted to show that this effect does exist and we desired to know the behaviour of these types of reflections and transmissions in contrast with reflections and transmissions from a discrete boundary.

Acknowledgements

I would like to thank Dr. Douglas R. Schmitt of the University of Alberta for his interest in and support of my research over the last year as my supervisor and for being willing to supervise me after my previous supervisor, Dr. F. Hron, unfortunately passed away.

Dr. Jeremy Gallop, Dr. Mauricio Sacchi, and Joseph Molyneux I would like to thank for our many fruitful discussions on seismology and computation.

I extend my gratitude to the members of my examining committee for their constructive suggestions and for agreeing to read my thesis.

I owe a debt to all of my friends and colleagues for their support and encouragement. I would specifically like to thank Kipp Cannon, Dr. Philip Kayal, Dr. Anthony Faust, Dr. Andrew Brown, Norm Buchanan, Henning Kühl, and Patrick Sutton for all of their help with the LaTeX document preparation system. I would also like to thank the Physics Coffee Company for keeping me well fueled during the course of my study.

NSERC funded the research contained within this thesis with a PGS-A grant.

Finally, I would espescially like to thank my parents for igniting the fuse of scientific curiousity within me and for always having confidence in me.

Contents

1 Introduction **1**

2 Asymptotic Ray Theory in Three Dimensionally Inhomogeneous Isotropic Media **5**

2.1 Introduction to Asymptotic Ray Theory 5

2.2 The Kinematic and Dynamic Properties of a Ray 7

2.2.1 The Eikonal Equations 8

2.2.2 Zeroth Order Amplitudes for P-waves 10

2.2.3 Zeroth Order Amplitudes for S-waves 12

2.2.4 Higher Order Amplitudes for P-Waves 15

2.2.5 Higher Order Amplitudes for S-Waves 16

2.3 Boundary Conditions 19

2.3.1 The Concept of an Interface 19

2.3.2 Kinematic Boundary Conditions 20

2.3.3 Dynamic Boundary Conditions 23

3 Dynamic Ray Tracing **29**

3.1 Geometrical Spreading 29

3.2 Evaluation of Geometrical Spreading in a continuously varying medium . 30

3.3 Boundary Conditions on the Curvature of a Wavefront 33

3.4 Gel'chinskiy's Equations 37

4 Modelling the Effect of Velocity Gradients in the Change in Geometrical Spreading Across a Boundary **43**

4.1 Introduction 43

4.2 Ray Tracing in a Constant Gradient Medium 45

4.2.1 Ray Paths 45

4.2.2 Geometrical Spreading 48

4.3 The Effect of a Boundary 51

4.3.1 Amplitude Versus Offset Curves for Constant Gradient Media . . 51

4.3.2 Comparison of Analytical Calculations with the Ray Shooting Method to Determine Geometrical Spreading 64

5 Reflections from a Second Order Discontinuity **68**

5.1 Introduction 68

5.2 Boundary Conditions 69

5.3 First Order Reflected and Transmitted Waves 73

6 Conclusions **79**

List of Figures

2.1 The ray coordinates (s, γ_1, γ_2) for a point on a ray in relation to the Cartesian coordinates. The source is at the origin. 11

2.2 The point of incidence of a ray on a boundary, Σ. The plane of incidence is also shown. 20

3.1 A diagram of the (l, q_1, q_2) coordinate system as compared to the (s, q_1, q_2) coordinate system. The point $\tau(s, q_1, q_2)$ may be found from $\tau(s, 0, 0)$ by equation 3.15. 34

3.2 The unit vectors for the ray centered coordinate system and Gel'chinskiy's equations for an incident and a reflected ray near a boundary Σ in the plane of incidence. 38

4.1 Velocities from PREM of Dziewonski and Anderson [12]. The velocity profile for P- and S- waves contain discontinuities with gradients on either side. 44

4.2 The coordinate systems used for a ray propagating in a medium with a constant gradient. 46

4.3 A plot of the arrivals examined in this section. The dashed rays denote shear waves and the solid rays denote P-waves. 53

4.4 The Mississippi Model. 54

4.5 Rays for the primary non-phase converted reflection in the Mississippi Model. 55

4.6 The calculated vertical component amplitudes of reflected and transmitted arrivals from an isotropic point source located on the surface of the Mississippi Model recorded at a receiver on the surface. The difference in amplitude of the two curves in each plot is due to inclusion or exclusion of the effects of velocity gradients on the jump in geometrical spreading across the boundary at 800 m. 56

4.7 The calculated horizontal component amplitudes of reflected and transmitted arrivals from an isotropic point source located on the surface of the Mississippi Model recorded at a receiver on the surface. The difference in amplitude of the two curves in each plot is due to inclusion or exclusion of the effects of velocity gradients on the jump in geometrical spreading across the boundary at 800 m. 57

4.8 The Negative Gradient Model. 59

4.9 Rays for the primary non-phase converted reflection in the Negative Gradient Model. 60

4.10 The calculated vertical component amplitudes of reflected and transmitted arrivals from an isotropic point source located on the surface of the Negative Gradient Model recorded at a receiver on the surface. The difference in amplitude of the two curves is due to inclusion or exclusion of the effects of velocity gradients on the jump in geometrical spreading across the boundary at 100 m. 62

4.11 The calculated horizontal component amplitudes of reflected and transmitted arrivals from an isotropic point source located on the surface of the Negative Gradient Model recorded at a receiver on the surface. The difference in amplitude of the two curves is due to inclusion or exclusion of the effects of velocity gradients on the jump in geometrical spreading across the boundary at 100 m. 63

4.12 A comparison of different calculations of geometrical spreading in the Negative Gradient Model for the P1P1 arrival as recorded at the surface. The two curves represent the numerator of the ratio being equal to the analytic geometrical spreading evaluated by either including or excluding the 3rd term in equation 3.24. 65

4.13 A comparison of the complete analytical geometrical spreading with the ray-shooting geometrical spreading in the Negative Gradient Model for the P1P1 arrival as recorded at the surface. 66

5.1 The Červený Model. 70

5.2 Amplitude versus angle curves for first order reflections from the second order discontinuity in the Červený model where $r_o = 150$m. 73

5.3 Amplitude versus angle curves for first order reflections from the second order discontinuity in the Červený model where $r_o = 1500$m. 75

5.4 Amplitude versus angle curves for first order reflections from the second order discontinuity in the Červený model where $r_o = 15000$m. 76

5.5 Reflection/transmission coefficient versus r_o for the Červený Model. The angle of incidence is 45°. 78

CHAPTER 1

Introduction

Forward modelling of a wavefield response is one of the most important tools in seismology. The simulated seismic response of an appropriate model of the Earth is calculated and then compared to the actual observations. This is a powerful way to help confirm whether a hypothesized structure truly exists. Traditionally, only the traveltimes are modelled but accurate value amplitudes on these synthetic wavefronts are increasingly desired. Determining how a wave may behave dynamically (i.e. as it propagates) is becoming as important a tool as knowing the kinematic properties of the wave (i.e.where and when in propagates). This is critical today as we seek to determine increasing finer details about the Earth's structure.

Usually, many models of the Earth consider it to be laminated consisting of layers of constant seismic velocity. This fiction is not entirely realistic. In many circumstances, the velocity may change gradually. Some examples of this are the progressive increase in speed in thick shale sequences due to overburden pressure and diagenesis, the gradual increase in velocity between the 400 and 660 km discontinuities, and the inferred gradual change over a finite distance of the discontinuities themselves as solid state phase transforms to higher pressure forms. As such, many geological models of the Earth contain vertical gradients in the propagation velocity. One strategy of handling these gradients is to divide a given medium into homogeneous horizontal thin slices with incrementally varying material properties. This

method gives reasonable results for the traveltime of the wave but it is deficient for predicting accurate amplitudes. Therefore, an investigation into how gradients in material properties affect the observed seismic amplitudes is the primary contribution of this thesis.

If a wave has sufficiently high frequency, we can say that the energy of a wavefront is carried by a ray (i.e. a curve in space). This ray is oriented perpendicular to the wavefront in an isotropic medium. The particle displacement amplitude for the ray may then be expressed as an asymptotically convergent series using Asymptotic Ray Theory (ART). Analytic formulae for approximating these amplitudes are obtained by truncating this series. ART, which will be reviewed in Chapter 2 of this thesis, has been successful in predicting various phenomena not found with the conventional plane wave approximations. These phenomena include head waves [6], transverse motion propagating from an explosive source near a surface [18], and longitudinal or transverse wavefronts not carrying pure longitudinal or pure transverse motions [19]. While I will only be summarizing the development of the theory for isotropic elastic media, it has been extended to visco-elastic media [23] and anisotropic media [33], [31].

There are complications when a wave travels in a generally inhomogeneous medium with curved boundaries. One of these complications is that the wavefronts do not have the simple geometries that would be observed in homogeneous media separated by plane boundaries. For such a case, a complete evaluation of the leading term in the ray series has to be facilitated using dynamic ray tracing. Dynamic ray tracing allow for the curvature of a wavefront to be evaluated everywhere along a ray. This theory, reviewed in Chapter 3, accounts for the fact that the amplitude

along a ray depends on changes in the wavefront shape. In the same chapter, we will also prove that two methods employed for describing the change in shape of a wavefront as it encounters a boundary, one derived from dynamic ray tracing by Červený and Hron [5] and the other derived using the principles of differential geometry by Gel'chinskiy [14], are equivalent.

The results are then used in Chapter 4 to show how seismic energy is focussed or defocussed by the local velocity gradients in the vicinity of a boundary. Dynamic ray tracing predicts that the shape of a partitioned wavefront depends on these local velocity gradients. Our analytical results will be compared against a well established approximation in order to assess their validity.

Chapter 5 is devoted to showing that a discrete change in material properties is not necessary in order to partition seismic energy. The theory so developed suggests that a simple change in the velocity gradient with depth will scatter seismic energy. Such a change is called a first order discontinuity because there is a discontinuity in the first order derivative of a material property, in this case velocity. Some examples of this are given to show that many factors influence this special case of reflectivity.

The new work in this thesis is primarily devoted to exploring how velocity gradients influence the amplitudes we observe. It is well known that within the Earth, velocity gradients are commonplace so their exact effect on the seismic signals is a very necessary piece of information. In some Earth models changes in the velocity gradient do exist. For example, in the mantle transition zone and at the lower mantle-D" discontinuity in PREM [27], such discontinuities exist. The

nature of the partitioned rays would be of interest in any potential study of these discontinuities.

CHAPTER 2

Asymptotic Ray Theory in Three Dimensionally Inhomogeneous Isotropic Media

2.1 Introduction to Asymptotic Ray Theory

Asymptotic Ray Theory (ART) applied to the elastodynamic equation was first developed by Soviet scientists such as Babich and Alekseev [2] and later, though probably independently, by Karal and Keller [22] in the USA. A rigorous discussion of ART is contained in Červený and Ravindra's [6] classic book and in papers such as Hron and Kanasewich [17] and Červený and Hron [5]. Essentially, ART is used to predict the amplitude variations along a ray, being the orthogonal trajectory of a wavefront, in a more accurate manner than simple geometrical arguments. In the high frequency limit, the ART solution converges to the solution predicted from geometrical ray theory.

As ART is a high frequency approximation, it may not be used for certain types of media where scale lengths are much less than a seismic wavelength. Also, in the vicinity of a caustic, on the boundary of a shadow zone, or in the interference zone between a head wave and a reflected wave, other techniques must be employed to approximate the wavefield. However, the advantage that ART has over full wave solution (i.e. finite-difference) is speed of computation and analytic solutions

which provide phyical insight into seismic wave propagation. ART is also a better approximation than geometrical ray solutions as certain 'non-geometrical' effects are detected by ART. These effects include head waves, tunnelling waves through higher velocity medium, S^* waves propagating from an explosive source near an interface with transverse polarization, and depolarization of seismic waves. A summary of these effects is found in the paper by Babich and Kiselev [3]

Suppose we have an isotropic medium described by elastic parameters λ, μ (the Lamé parameters), and ρ (the mass density) belonging to the C^∞ family of functions. C^∞ indicates the set of functions which are not only continuous, but are continuous in all spatial derivatives. In such a medium, the elastodynamic equation has the form:

$$\begin{aligned} \rho\frac{\partial^2\vec{W}}{\partial t^2} &= (\lambda+\mu)\vec{\nabla}(\vec{\nabla}\cdot\vec{W}) + \mu\vec{\nabla}^2\vec{W} + \vec{\nabla}\lambda(\vec{\nabla}\cdot\vec{W}) + \vec{\nabla}\mu\times(\vec{\nabla}\times\vec{W}) \\ &\quad + 2(\vec{\nabla}\mu\cdot\vec{\nabla})\vec{W} \end{aligned} \tag{2.1}$$

where $\vec{W}$ is the particle displacement and t is the time. We shall seek solutions to equation 2.1 in the form of an asymptotic expansion

$$\vec{W} = \sum_{k=0}^{\infty} \vec{W}_k f_k(t-\tau) \tag{2.2}$$

that is convergent for high frequency signals. The function τ is the traveltime to a wavefront, f_k is a function with the property

$$\frac{d\, f_k(t-\tau)}{d(t-\tau)} = f_{k-1}(t-\tau) \quad (k \geq 1) \tag{2.3}$$

and $\vec{W}_k$ is referred to as the kth order amplitude term. Equation 2.2 can be thought of as an extension of a plane wave approximation with higher order perturbations

and incorporating the slow variation of the wavefield in the $\vec{W}_k$ terms . Another important feature of equation 2.2 is that the time dependence is contained only in the f_k terms. Both the amplitude and phase terms are only functions of space.

The f_k functions are easily determined when we consider that f_o is simply the shape of the source wavelet. Integration of this source wavelet will determine all of the other f_k's. Frequently, the time dependence of the source is assumed to be harmonic so that $f_o = e^{i\omega t}$ where ω is the frequency. In this case, the expansion will have the form

$$\vec{W} = e^{i\omega t} \sum_{k=0}^{\infty} (i\omega)^{-k} \vec{W}_k. \tag{2.4}$$

However, the source wavelet, $f_o(t)$, may, in general, contain any arbitrary degree of discontinuity at $t = 0$.

2.2 The Kinematic and Dynamic Properties of a Ray

Upon application of the ray series expansion 2.2 to the inhomogeneous elastodynamic equation 2.1 we obtain the following recurrence relation:

$$\vec{N}(\vec{W}_{k+2}) - \vec{M}(\vec{W}_{k+1}) + \vec{L}(\vec{W}_k) = 0 \quad (k \geq -2) \tag{2.5}$$

where we define $\vec{W}_{-2} \equiv \vec{W}_{-1} \equiv 0$ to remain consistent. The vector operators $\vec{N}$, $\vec{M}$, and $\vec{L}$ are defined as:

$$\vec{N}(\vec{u}) \;=\; (\lambda + \mu)(\vec{\nabla}\tau \cdot \vec{u})\vec{\nabla}\tau + \left[\mu(\vec{\nabla}\tau)^2 - \rho\right] \vec{u}, \tag{2.6}$$

$$\vec{M}(\vec{u}) = (\lambda+\mu)\left[(\vec{\nabla}\cdot\vec{u})\vec{\nabla}\tau + \vec{\nabla}(\vec{u}\cdot\vec{\nabla}\tau)\right] + \mu\left[(\vec{\nabla}^2\tau)\vec{u} + 2(\vec{\nabla}\tau)^2\frac{d\vec{u}}{d\tau}\right] + (\vec{u}\cdot\vec{\nabla}\tau)\vec{\nabla}\lambda + (\vec{\nabla}\mu\cdot\vec{u}) + (\vec{\nabla}\mu\cdot\vec{\nabla}\tau)\vec{u}, \text{ and} \quad (2.7)$$

$$\vec{L}(\vec{u}) = (\lambda+\mu)\vec{\nabla}(\vec{\nabla}\cdot\vec{u}) + \mu\vec{\nabla}^2\vec{u} + \vec{\nabla}\lambda(\vec{\nabla}\cdot\vec{u}) + \vec{\nabla}\mu\times(\vec{\nabla}\times\vec{u}) + 2(\vec{\nabla}\mu\cdot\vec{\nabla})\vec{u}. \quad (2.8)$$

2.2.1 The Eikonal Equations

We may glean the various kinematic and dynamic properties of the ray, in the high frequency limit from equation 2.5. Specifically, if we examine the case where $k = -2$ and keeping in mind that $\vec{W}_{-2} \equiv \vec{W}_{-1} \equiv 0$ then we obtain the eikonal equation:

$$\vec{N}(\vec{W}_o) = 0. \quad (2.9)$$

We may rewrite this equation as an eigenvalue problem by defining a matrix $\mathbf{N}$ with components:

$$N_{ij} = \frac{\lambda+\mu}{\mu}p_i p_j - \delta_{ij}\frac{\rho}{\mu} \quad (2.10)$$

where p_i are the components of the slowness vector, $\vec{p} = \vec{\nabla}\tau$, and δ_{ij} is the Krönecker delta. Equation 2.9 then becomes:

$$\mathbf{N}\cdot\vec{W}_o = -|\vec{\nabla}\tau|^2\vec{W}_o. \quad (2.11)$$

Due to the Hermiticity of the $\mathbf{N}$ matrix, equation 2.11 gives rise to three real, mutually orthogonal eigenvectors, $\vec{g}_j$, associated with three eigenvalues, $-\Lambda_j = |\vec{\nabla}\tau|^2$.

Each eigenvector will be associated with a particular particle motion which propagates at a speed determined by the eigenvalue. We may solve for these eigenvalues by finding the roots of the equation

$$\det(\mathbf{N} - \Lambda\mathbf{I}) = -\frac{[\mu\Lambda + \rho]^2[(\lambda + 2\mu)\Lambda + \rho]}{\mu^3} = 0. \tag{2.12}$$

Equation 2.12 has a double root indicating

$$|\vec{\nabla}\tau| = \sqrt{\frac{\mu}{\rho}} = v_s \tag{2.13}$$

and a single root that indicates

$$|\vec{\nabla}\tau| = \sqrt{\frac{\lambda + 2\mu}{\rho}} = v_p. \tag{2.14}$$

Equations 2.13 and 2.14 are known as the eikonal equations and we may utilize them to determine the path of propagation of the wave, the raypath, via variational calculus or some sort of finite difference method. These equations also serve to determine the speed of propagation of a ray, given as v_s or v_p for each mode of propagation. Thus, we can see that the eikonal equation serves to specify all of the kinematic properties of a ray.

The double root of equation 2.12 indicates that the associated eigenvectors for this eigenvalue cannot be uniquely determined. These vectors exist in a plane perpendicular to the raypath and are called shear waves (S-waves) due to the transverse particle motion. This result is a consequence of equation 2.9 which requires the zeroth order particle displacement vector, $\vec{W}_o^{(s)}$, to be perpendicular to $\vec{\nabla}\tau$, which is aligned in the direction of propagation. The other type of motion, longitudinal waves (P-waves) are characterized by a particle motion vector, $\vec{W}_o^{(p)}$, along the ray.

2.2.2 Zeroth Order Amplitudes for P-waves

In the previous section, we have seen how all the kinematic properties of a ray may be determined when we examine equation 2.5 for the case of $k = 0$. Next, we will look at this equation for P-waves ($\vec{\nabla}^2\tau = v_p^{-2}$) at $k = 1$ in order to glean some information about the dynamic properties (i.e. the amplitudes) of a ray. Therefore,

$$\vec{N}(\vec{W}_1^{(p)}) = \vec{M}(\vec{W}_o^{(p)}). \tag{2.15}$$

The component of equation 2.15 parallel to the propagation direction must be zero for P-waves. Thus, we may define a new operator, $M_{\|}$, such that:

$$M_{\|}(\vec{u}) = v_p\vec{\nabla}\tau_p \cdot \vec{M}(\vec{u}) \text{ and} \tag{2.16}$$

$$M_{\|}(\vec{W}_o^{(p)}) = 2\sqrt{\left(\frac{\rho}{v_s J}\right)}\frac{d}{d\tau}\left[\sqrt{(\rho v_s J)}W_o^{(p)}\right] = 0 \tag{2.17}$$

where $W_o^{(p)}$ is the projection of $\vec{W}_o^{(p)}$ in the direction of propagation and J is the Jacobian of the transformation from Cartesian coordinates to ray coordinates and it will be discussed in more detail in the next chapter. The J function enters the equation as evaluation of $M_{\|}$ involves taking the Laplacian of the function τ and

$$\vec{\nabla}^2\tau = \frac{1}{Jv}\frac{d}{d\tau}\left(\frac{J}{v}\right). \tag{2.18}$$

The basis of the ray coordinates is given as $(\hat{s},\ \hat{\gamma}_1,\ \hat{\gamma}_2)$ such that s specifies an arclength on the ray and γ_1 and γ_2 are the take off angles of a given ray as shown in Figure 2.1. This function J is also a measure of the geometrical divergence of a ray tube, an infinitesimally narrow pencil of rays around a central ray, and it will be examined in more detail in the next chapter.

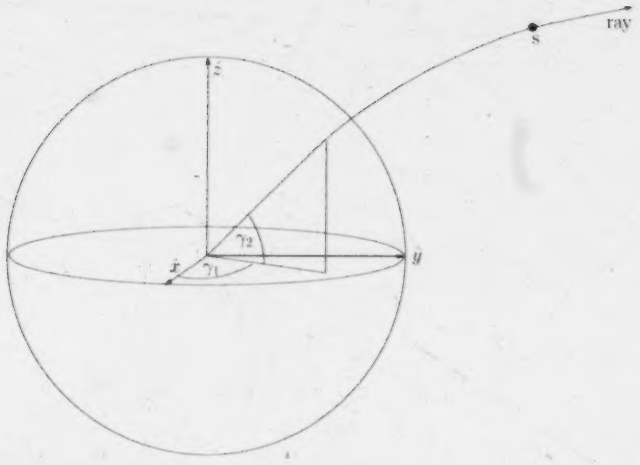

Figure 2.1: The ray coordinates (s, γ_1, γ_2) for a point on a ray in relation to the Cartesian coordinates. The source is at the origin.

The solution to equation 2.17 is immediately apparent as

$$W_o^{(p)} = \left(\frac{\rho_o v_{po}}{\rho v_p}\right)^{\frac{1}{2}} \frac{P_o}{(J/J_o)^{\frac{1}{2}}} \tag{2.19}$$

where the quantities $\rho_o = \rho(\tau_o)$, $v_{po} = v_p(\tau_o)$, $J_o = J(\tau_o)$, and $P_o = W_o^{(p)}(\tau_o)$ are measured at a reference traveltime, τ_o, along the ray. In the equation, there exists a term $(J/J_o)^{\frac{1}{2}}$ which is frequently called the geometrical spreading, L. Hron [16] noted that equation 2.19 may be obtained by considering that the seismic energy in a ray tube is conserved.

2.2.3 Zeroth Order Amplitudes for S-waves

The same basic analysis as used in the previous section may be used for the problem of zeroth order amplitudes for S-waves. A complication arises, however, as the direction of particle displacement is only confined to a plane and the displacement vector is free to rotate around the ray in this plane. The derivation of the magnitude of displacement, however, may be solved in a somewhat analogous technique to the solution for zeroth order P-waves.

We know from equation 2.5 that

$$\vec{N}(\vec{W}_1^{(s)}) = \vec{M}(\vec{W}_o^{(s)}) \tag{2.20}$$

and from equation 2.6 that a component of the $\vec{N}$ operator perpendicular to the ray is zero for shear waves. The amplitude for the zeroth order shear term may be written as:

$$\vec{W}_o^{(s)} = W_o^{(s)} \cdot \hat{\epsilon}_\perp \tag{2.21}$$

where $\hat{\epsilon}_\perp$ is the unit vector aligned along the direction of particle displacement. This unit vector may then be used to define a new operator, $M_\perp = \vec{M} \cdot \epsilon_\perp$ and, in conjunction with equation 2.20, we obtain:

$$M_\perp(\vec{W}_o^{(s)}) = 2\sqrt{\left(\frac{\rho}{v_s J}\right)}\frac{d}{d\tau}\left[\sqrt{(\rho v_s J)}W_o^{(s)}\right] = 0. \tag{2.22}$$

This equation may be solved like equation 2.17 to obtain

$$W_o^{(s)} = \left(\frac{\rho_o v_{so}}{\rho v_s}\right)^{\frac{1}{2}} \frac{S_o}{(J/J_o)^{\frac{1}{2}}}. \tag{2.23}$$

The terms $v_{so} = v_s(\tau_o)$ and $S_o = \vec{W}_o^{(s)}(\tau_o)$ are measured, similar to analogous terms in equation 2.19, at a traveltime τ_o on the ray.

The problem of the magnitude of zeroth order shear wave amplitude being solved, we may examine the more complex case of determining the direction of the particle displacement. To do this, we need to use the three basis vectors for a curve from differential geometry. These are $\hat{t}$, the tangent vector, $\hat{n}$, the normal vector, and $\hat{b}$, the binormal vector. These vectors are related through a set of three formulae known as the Frenet formulae [11]:

$$\begin{aligned} \frac{d\hat{t}}{ds} &= K\hat{n}, \\ \frac{d\hat{n}}{ds} &= -K\hat{t} + T\hat{b}, \text{ and} \\ \frac{d\hat{b}}{ds} &= -T\hat{n}. \end{aligned} \tag{2.24}$$

In these equations 2.24, K is the curvature of the ray, T is the torsion of the ray, and s is a measure of arclength. In this orthonormal basis,

$$\vec{W}_o^{(s)} = W_{on}^{(s)}\hat{n} + W_{ob}^{(s)}\hat{b} \text{ and} \tag{2.25}$$

$$\hat{\epsilon}_\perp = \cos\phi\hat{n} + \sin\phi\hat{b} \tag{2.26}$$

where ϕ is the angle between the normal vector and $W_o^{(s)}$. The use of this basis allows us to define two new vector operators:

$$M_n(\vec{W}_o^{(s)}) = \vec{M}(\vec{W}_o^{(s)}) \cdot \hat{n} = 0 \text{ and} \tag{2.27}$$

$$M_b(\vec{W}_o^{(s)}) = \vec{M}(\vec{W}_o^{(s)}) \cdot \hat{b} = 0. \tag{2.28}$$

Using equation 2.25 and the Frenet formulae, 2.24, equations 2.27 and 2.28 become:

$$M_n(\vec{W}_o^{(s)}) = \frac{\mu}{v_s^2}\left[v_s W_{on}^{(s)}\vec{\nabla}^2\tau + 2\left(\frac{dW_{on}^{(s)}}{d\tau} - v_s T W_{ob}^{(s)}\right) + \frac{W_{on}^{(s)}}{\mu}\frac{d\mu}{dt}\right] \text{ and} \quad (2.29)$$

$$M_b(\vec{W}_o^{(s)}) = \frac{\mu}{v_s^2}\left[v_s W_{ob}^{(s)}\vec{\nabla}^2\tau + 2\left(\frac{dW_{ob}^{(s)}}{d\tau} + v_s T W_{on}^{(s)}\right) + \frac{W_{ob}^{(s)}}{\mu}\frac{d\mu}{dt}\right]. \quad (2.30)$$

Knowing that $W_{on}^{(s)} = W_o^{(s)}\cos\phi$ and $W_{ob}^{(s)} = W_o^{(s)}\sin\phi$, the two coupled equations above, 2.29 and 2.30 may be reduced to a single first order differential equation in ϕ:

$$\frac{d\phi}{d\tau} = -v_s T \quad (2.31)$$

giving the orientation of the shear polarization vector as:

$$\phi(\tau) = -\int_{\tau_o}^{\tau} v_s T d\tau + \phi(\tau_o) \quad (2.32)$$

What this result tells us is that the polarization vector of a zeroth order shear wave rotates about the ray according to the amount of torsion exhibited by the ray. For the case of inhomogeneity existing in only one direction, such as the case of a spherically symmetric earth, the rays are plane curves and therefore have no torsion. In these cases, the shear wave polarization does not change along the ray and it is said to be preserved.

Comparison of equation 2.32 and the third Frenet formula, $\frac{d\hat{b}}{ds} = -T\hat{n}$, reveals that the shear wave polarization rotates about the ray with the same speed as the normal and binormal vectors. Thus, these vectors provide a basis in which the orientation of the $\vec{W}_o^{(s)}$ vector is constant.

2.2.4 Higher Order Amplitudes for P-Waves

It now remains to examine the case where $k \geq 0$ in equation 2.5. We will discover that there is no guarantee that the higher order P-wave amplitude vector, $\vec{W}_k^{(p)}$, is aligned along the ray. It makes sense then, to define the principal compqnent of amplitude, $\vec{W}_{k\|}^{(p)}$ as the component of $\vec{W}_k^{(p)}$ aligned along the ray. Also, we must define $\vec{W}_{k\perp}^{(p)}$, the additional component, as $\vec{W}_{k\perp}^{(p)} = \vec{W}_k^{(p)} - \vec{W}_{k\|}^{(p)}$.

The projection of equation 2.5 in the plane of propagation must be used in order to obtain useful formulae for the higher order amplitudes. It is useful, then, to define the operators

$$\vec{N}_{\|}(\vec{u}) = (\vec{N}(\vec{u}) \cdot v_p \vec{\nabla}\tau) v_p \vec{\nabla}\tau, \tag{2.33}$$

$$\vec{M}_{\|}(\vec{u}) = (\vec{M}(\vec{u}) \cdot v_p \vec{\nabla}\tau) v_p \vec{\nabla}\tau \text{ and} \tag{2.34}$$

$$\vec{L}_{\|}(\vec{u}) = (\vec{L}(\vec{u}) \cdot v_p \vec{\nabla}\tau) v_p \vec{\nabla}\tau. \tag{2.35}$$

It is easily verified that

$$\vec{N}(\vec{W}_k^{(p)}) = \rho \left(\frac{(v_s^2 - v_p^2)}{v_p^2} \right) \vec{W}_{k\perp}^{(p)}. \tag{2.36}$$

Therefore, it is possible to solve for the additional component, $\vec{W}_{k\perp}^{(p)}$, with the aid of equation 2.5 as

$$\vec{W}_{k\perp}^{(p)} = \frac{v_p^2}{\rho(v_s^2 - v_p^2)} \left[\vec{M}(\vec{W}_{k-1}^{(p)}) - \vec{L}(\vec{W}_{k-2}^{(p)}) \right]. \tag{2.37}$$

The principal component may be solved for if we realize that

$$\vec{N}_{\|}(\vec{W}_k^{(p)}) = 0. \tag{2.38}$$

This allows the component parallel to the ray of equation 2.5 to be written as

$$\vec{M}_{\|}(\vec{W}_{k}^{(p)}) - \vec{L}_{\|}(\vec{W}_{k-1}^{(p)}) = 0. \tag{2.39}$$

As $\vec{M}$ is a linear operator, and recalling equation 2.17, we may write

$$\begin{aligned} \vec{M}_{\|}(\vec{W}_{k\|}^{(p)}) &= \vec{L}_{\|}(\vec{W}_{k-1}^{(p)}) - \vec{M}_{\|}(\vec{W}_{k\perp}^{(p)}) \\ &= 2\sqrt{\left(\frac{\rho}{v_p J}\right)}\frac{d}{d\tau}\left[\sqrt{(\rho v_s J)}W_{k\|}^{(p)}\right]. \end{aligned} \tag{2.40}$$

Equation 2.40 may be solved as a first order linear ordinary differential equation with solution:

$$\begin{aligned} \vec{W}_{k\|}^{(p)} = \frac{1}{(\rho v_p J)^{\frac{1}{2}}}\Bigg[\int_{\tau_o}^{\tau}\frac{v_p}{2}\left(\frac{v_p J}{\rho}\right)^{\frac{1}{2}}\left(\vec{L}_{\|}(\vec{W}_{k-1}^{(p)}) - \vec{M}_{\|}(\vec{W}_{k\perp}^{(p)})\right)\cdot\vec{\nabla}\tau' d\tau' \\ + (\rho_o v_{po} J_o)^{\frac{1}{2}}\vec{P}_k\Bigg] \end{aligned} \tag{2.41}$$

where $\vec{P}_k$ is equal to $\vec{W}_{k\|}^{(p)}$ measured at a time τ_o and the integration is carried out along the ray.

2.2.5 Higher Order Amplitudes for S-Waves

We may employ analogous techniques to those used in the previous section to obtain equations describing the higher order amplitudes of P-waves. The higher order amplitude vector, $\vec{W}_{k}^{(s)}$, can be split into a principal component, $\vec{W}_{k\perp}^{(s)}$, in the normal plane of the ray, and an additional component, $\vec{W}_{k\|}^{(s)}$ aligned along the ray. As in the previous section, we shall first devote ourselves to deriving an expression for the additional component of $\vec{W}_{k}^{(s)}$. Knowing that

$$\vec{N}(\vec{W}_{k}^{(s)}) = \rho\left(\frac{(v_p^2 - v_s^2)}{v_s^2}\right)\vec{W}_{k\|}^{(s)}, \tag{2.42}$$

we may use equation 2.5 to obtain the following expression for the additional component of the S-wave:

$$\vec{W}_{k\|}^{(s)} = \frac{v_s^2}{\rho(v_p^2 - v_s^2)} \left[\vec{M}(\vec{W}_{k-1}^{(s)}) - \vec{L}(\vec{W}_{k-2}^{(s)})\right]. \tag{2.43}$$

The derivation of the principal component for the higher order S-wave amplitude is more complicated than the corresponding term for higher order P-waves. This is due to the orientation of the vector only being confined to a plane. We will need to decompose the $\vec{W}_{k\perp}^{(s)}$ vector into components aligned along the normal, $\hat{n}$, and binormal, $\hat{b}$, directions of the ray. To help us with this derivation, we shall need to define the operators

$$\vec{N}_n(\vec{u}) = (\vec{N}(\vec{u}) \cdot \hat{n})\hat{n}, \tag{2.44}$$

$$\vec{M}_n(\vec{u}) = (\vec{M}(\vec{u}) \cdot \hat{n})\hat{n}, \tag{2.45}$$

$$\vec{L}_n(\vec{u}) = (\vec{L}(\vec{u}) \cdot \hat{n})\hat{n}, \tag{2.46}$$

$$\vec{N}_b(\vec{u}) = (\vec{N}(\vec{u}) \cdot \hat{b})\hat{b}, \tag{2.47}$$

$$\vec{M}_b(\vec{u}) = (\vec{M}(\vec{u}) \cdot \hat{b})\hat{b}, \text{ and} \tag{2.48}$$

$$\vec{L}_b(\vec{u}) = (\vec{L}(\vec{u}) \cdot \hat{b})\hat{b}. \tag{2.49}$$

For any shear wave, $\vec{N}_n(\vec{W}_{k\perp}^{(s)}) = \vec{N}_b(\vec{W}_{k\perp}^{(s)}) = 0$. Therefore, taking the normal and binormal components of equation 2.5 and exploiting the fact that the vector operators are linear results in:

$$\vec{M}_n(\vec{W}_{k\perp}^{(s)}) = \vec{L}_n(\vec{W}_{k-1}^{(s)}) - \vec{M}_n(\vec{W}_{k\|}^{(s)}) \text{ and} \tag{2.50}$$

$$\vec{M}_b(\vec{W}_{k\perp}^{(s)}) = \vec{L}_b(\vec{W}_{k-1}^{(s)}) - \vec{M}_b(\vec{W}_{k\|}^{(s)}). \tag{2.51}$$

With the aid of equations 2.29 and 2.30 we have a set of two coupled equations for the normal and binormal components of $\vec{W}_{k\perp}^{(s)}$ ($W_{kn}^{(s)} = \vec{W}_{kn}^{(s)} \cdot \hat{n}$ and $W_{kb}^{(s)} = \vec{W}_{kb}^{(s)} \cdot \hat{b}$

respectively) given as:

$$\begin{aligned}
\vec{M}_n(\vec{W}^{(s)}_{k\perp}) &= \frac{\mu}{v_s^2}\left[v_s W^{(s)}_{kn}\vec{\nabla}^2\tau + 2\left(\frac{dW^{(s)}_{kn}}{d\tau} - v_s T W^{(s)}_{kb}\right) + \frac{W^{(s)}_{kn}}{\mu}\frac{d\mu}{dt}\right] \\
&= \vec{L}_n(\vec{W}^{(s)}_{k-1}) - \vec{M}_n(\vec{W}^{(s)}_{k\|}) \text{ and} \qquad (2.52) \\
\vec{M}_b(\vec{W}^{(s)}_{k\perp}) &= \frac{\mu}{v_s^2}\left[v_s W^{(s)}_{kb}\vec{\nabla}^2\tau + 2\left(\frac{dW^{(s)}_{kb}}{d\tau} + v_s T W^{(s)}_{kn}\right) + \frac{W^{(s)}_{kb}}{\mu}\frac{d\mu}{dt}\right] \\
&= \vec{L}_b(\vec{W}^{(s)}_{k-1}) - \vec{M}_b(\vec{W}^{(s)}_{k\|}). \qquad (2.53)
\end{aligned}$$

We may simplify these two formulae by adopting the use of complex notation in order to keep track of $W^{(s)}_{kn}$ and $W^{(s)}_{kb}$ simultaneously. This is done by introducing a complex scalar, T_k, such that

$$T_k = W^{(s)}_{kn} + iW^{(s)}_{kb}. \qquad (2.54)$$

Equations 2.52 and 2.53 are then reduced to a single complex equation:

$$\frac{dT_k}{d\tau} + \frac{d}{d\tau}\left[\ln\left(e^{-i\phi(\tau)}(\rho v_s J)^{\frac{1}{2}}\right)\right]T_k = \frac{1}{2\rho}\left[\mathcal{L}(\vec{W}^{(s)}_{k-1}) - \mathcal{M}(\vec{W}^{(s)}_{k\|})\right] \qquad (2.55)$$

where $\phi(\tau)$ is defined in equation 2.32 and $\mathcal{L}$ and $\mathcal{M}$ are complex operators given by

$$\begin{aligned}
\mathcal{L}(\vec{u}) &= \vec{L}_n(\vec{u})\cdot\hat{n} + i\vec{L}_b(\vec{u})\cdot\hat{b} \text{ and} \qquad (2.56) \\
\mathcal{M}(\vec{u}) &= \vec{M}_n(\vec{u})\cdot\hat{n} + i\vec{M}_b(\vec{u})\cdot\hat{b}. \qquad (2.57)
\end{aligned}$$

The solution to equation 2.55 is then given by

$$\begin{aligned}
T_k = \frac{e^{i\phi(\tau)}}{(\rho v_s J)^{\frac{1}{2}}}\Bigg[&\int_{\tau_o}^{\tau}\frac{e^{-i\phi(\tau)}}{2\rho}(v_s J\rho)^{\frac{1}{2}}\left(\mathcal{L}(\vec{W}^{(s)}_{k-1}) - \mathcal{M}(\vec{W}^{(s)}_{k\|})\right)d\tau' \\
&+ (\rho_o v_{so} J_o)^{\frac{1}{2}} T_{ko}\Bigg] \qquad (2.58)
\end{aligned}$$

where $T_{ko} = T_k(\tau_o)$ and we integrate along the ray. Taking the real and complex parts of T_k will give the values of $W_{kn}^{(s)}$ and $W_{kb}^{(s)}$ respectively.

2.3 Boundary Conditions

2.3.1 The Concept of an Interface

The previous section was devoted to describing the behaviour of waves in a medium that was described by elastic parameters belonging to the C^∞ family of functions (i.e. the Lamé coefficients and the density were not only continuous, but all of their spatial derivatives were also continuous). When a ray encounters a discontinuity in the kth derivative of λ, μ, or ρ, the coefficients in the ray series, $\vec{W}_k$ also become discontinuous. As certain conditions must hold at this discontinuity, like continuity of displacement and of normal stress components, reflected and transmitted waves must exist in order for these conditions to be satisfied. Following the notation of Červený and Ravindra [6], a surface which exhibits a discontinuity of the nth derivative of elastic parameters will be called an *interface of (n+1)th order.* A surface where the elastic parameters themselves are discontinuous is an *interface of first order.* Higher order interfaces are also referred to as weak interfaces in the literature. In reality, many interfaces are gradational in nature as one material gradually incorporates another material until the other material is all that remains. Such gradational interfaces consist of a pair of first order interfaces complimenting one another and their reflective properties have been studied by Gupta [15] and Richards [29] with low frequency approximations. The reflectivity of a single first order interface will be discussed in chapter 5 of this thesis using ART.

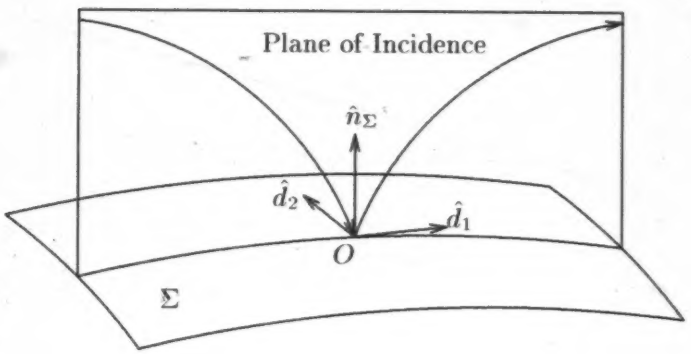

Figure 2.2: The point of incidence of a ray on a boundary, Σ. The plane of incidence is also shown.

2.3.2 Kinematic Boundary Conditions

Suppose the incident ray strikes the interface at the point O. The plane of incidence can then be defined as the plane that contains both the normal vector to the interface, Σ, and the tangent vector to the ray, $\hat{t}$ at the point O. The point, O, lies at the origin of a Cartesian coordinate system with a basis $(\hat{d}_1, \hat{d}_2, \hat{n}_\Sigma)$ where $\hat{n}_\Sigma$ is normal to the interface pointing into the first medium, $\hat{d}_1 \cdot \hat{t} \geq 0$, and $\hat{d}_1 \times \hat{d}_2 = \hat{n}_\Sigma$. Figure 2.2 shows the relationship between these unit vectors.

When examining the problem of reflection and transmission from a boundary, five waves are usually considered in the most general case — one incident, two reflected, and two transmitted. Therefore, we should adopt new notation in order to describe these waves. First, we will consider that locally, the interface divides the media into a first and a second medium. The elastic parameters in the first medium will be described by λ_1, μ_1, and ρ_1 whereas λ_2, μ_2, and ρ_2 will describe

these parameters in the second medium. The subscript, ν, will be employed to describe the type of wave — $\nu = 0$ will describe the incident wave (which can be either a P- or an S-wave in the following discussion), $\nu = 1$ and 2 will refer to the P- and S-waves in the first medium, and $\nu = 3$ and 4 will refer to the P- and S-waves in the second medium respectively. In addition, the S-waves have some degeneracy as they are only confined to a plane. In the following discussions, we may speak of S-waves polarized in the plane of incidence as SV-waves and S-waves polarized perpendicular to SV-waves parallel to the tangent plane of the boundary as SH-waves. We will write the ray expansion for the incident wave as

$$\vec{W}^o = \sum_{k=0}^{\infty} \vec{W}_k^o f_k(t - \tau_o) \tag{2.59}$$

and the reflected or transmitted wave's expansion will be

$$\vec{W}^\nu = \sum_{k=0}^{\infty} \vec{W}_k^\nu f_k(t - \tau_\nu). \tag{2.60}$$

In equations 2.59 and 2.60, the functions τ_o and τ_ν are the phase functions of the incident and resultant wavefronts, respectively, given as solutions to the eikonal equation, 2.13 or 2.14. At the interface,

$$\tau_o = \tau_\nu \tag{2.61}$$

for $\nu = 1, 2, 3, 4$.

In accordance with our new notation, we should designate the speed with which P-waves travel in the first medium, $v_1 = \alpha_1 = \sqrt{\frac{\lambda_1 + 2\mu_1}{\rho_1}}$; the speed of S-waves in the first medium will be $v_2 = \beta_1 = \sqrt{\frac{\mu_1}{\rho_1}}$; and $v_3 = \alpha_2 = \sqrt{\frac{\lambda_2 + 2\mu_2}{\rho_2}}$ and

$v_4 = \beta_2 = \sqrt{\frac{\mu_2}{\rho_2}}$ will denote P- and S- waves in the second medium respectively. Also, we can define

$$\gamma_i = \frac{\alpha_i}{\beta_i} = \sqrt{\frac{\mu_i}{\lambda_i + 2\mu_i}}; \quad i = 1, 2. \tag{2.62}$$

Naturally, the speed of the incident wave is given as v_o. In the following discussion, no restrictions will be placed on the type of incident wavefront or on the medium from which it originates.

We may use the eikonal equation, either 2.13 or 2.14, to determine the spatial derivatives of the phase function at the point, O, as

$$\tau_{\nu,1} = \tau_{o,1} = \frac{\sin\theta_\nu}{v_\nu}, \tag{2.63}$$

$$\tau_{\nu,2} = \tau_{o,2} = 0, \text{ and} \tag{2.64}$$

$$\tau_{\nu,n} = \pm\sqrt{v_\nu^{-2} - \tau_{\nu,1}^2} = \pm\sqrt{v_o^{-2} - \tau_{o,1}^2} \tag{2.65}$$

where $,_1$, $,_2$, and $,_n$ refer to directional derivatives in the d_1, d_2, and n directions respectively, θ_ν is the acute angle between the tangent of the νth ray and $\hat{n}$ at point O, and $\nu = 1, 2, 3, 4$. The directional derivative normal to the boundary, $\tau_{\nu,n}$ contains some ambiguity which may be resolved by considering which medium the ray is propagating in. Therefore

$$\tau_{\nu,n} = (-1)^{\epsilon_\nu + 1}\frac{\cos\theta_\nu}{v_\nu} \tag{2.66}$$

where

$$\epsilon_\nu = \begin{cases} 1, & \nu = 1, 2 \\ 2, & \nu = 3, 4 \end{cases} \tag{2.67}$$

and

$$\tau_{o,n} = (-1)^{\epsilon_o} \frac{\cos\theta_o}{v_o} \tag{2.68}$$

where ϵ_o is equal to 1 if the incident wave is propagating in the first medium and is equal to 2 if the wave is in the second medium.

In addition, for the case of supercritical refraction, $\tau_{o,1} > 1/v_\nu$, so $\sin\theta_\nu > 1$ and $\cos\theta_\nu = \pm i\sqrt{\sin^2\theta_\nu - 1}$. To resolve this sign ambiguity, we turn to the radiation condition stating that amplitude decays exponentially away from a boundary. Thus, the correct choice of sign yields

$$\cos\theta_\nu = -i\sqrt{\sin^2\theta_\nu - 1}, \quad \nu = 1, 2, 3, 4. \tag{2.69}$$

Equations 2.61, 2.63, 2.64, 2.66, and 2.69 together with the eikonal equation (2.14 for P-waves and 2.13 for S-waves) are enough to specify the kinematic properties of the rays diverging from the boundary. These equations uniquely determine the raypaths of all reflected and transmitted phases.

2.3.3 Dynamic Boundary Conditions

In order to specify the amplitudes of the various divergent waves from a boundary at the point, O, we must use the appropriate boundary conditions. These conditions consist of the normal stresses and the particle displacements being matched across a boundary. Formally, these conditions are:

$$\sum_{\nu=1}^{4} (-1)^{\epsilon_\nu} W^\nu_{(1)} = (-1)^{\epsilon_o + 1} W^o_{(1)} \,, \tag{2.70}$$

$$\sum_{\nu=1}^{4}(-1)^{\epsilon_\nu}W^{\nu}_{(2)} = (-1)^{\epsilon_o+1}W^{o}_{(2)} \ , \tag{2.71}$$

$$\sum_{\nu=1}^{4}(-1)^{\epsilon_\nu}W^{\nu}_{(n)} = (-1)^{\epsilon_o+1}W^{o}_{(n)} \ , \tag{2.72}$$

$$\sum_{\nu=1}^{4}(-1)^{\epsilon_\nu}\left[\lambda_{\epsilon_\nu}(\vec{\nabla}\cdot\vec{W}^{\nu}) + 2\mu_{\epsilon_\nu}W^{\nu}_{(n),n}\right] = (-1)^{\epsilon_o+1}\left[\lambda_{\epsilon_o}(\vec{\nabla}\cdot\vec{W}^{o}) + 2\mu_{\epsilon_o}W^{o}_{(n),n}\right] \ , \tag{2.73}$$

$$\sum_{\nu=1}^{4}(-1)^{\epsilon_\nu}\mu_{\epsilon_\nu}\left[W^{\nu}_{(1),n} + W^{\nu}_{(n),1}\right] = (-1)^{\epsilon_o+1}\mu_{\epsilon_o}\left[W^{o}_{(1),n} + W^{o}_{(n),1}\right] \ , \text{ and} \tag{2.74}$$

$$\sum_{\nu=1}^{4}(-1)^{\epsilon_\nu}\mu_{\epsilon_\nu}\left[W^{\nu}_{(2),n} + W^{\nu}_{(n),2}\right] = (-1)^{\epsilon_o+1}\mu_{\epsilon_o}\left[W^{o}_{(2),n} + W^{o}_{(n),2}\right] \ . \tag{2.75}$$

In equations 2.70-2.75, we have used a decomposition of the ray amplitudes in the boundary coordinates as

$$\vec{W}^{\nu} = W^{\nu}_{(1)}\hat{d}_1 + W^{\nu}_{(2)}\hat{d}_2 + W^{\nu}_{(n)}\hat{n}_\Sigma \ . \tag{2.76}$$

Terms in the ray series of the form $W^{\nu}_{k(1)}$, $W^{\nu}_{k(2)}$, and $W^{\nu}_{k(n)}$ may be defined in a similar manner.

We may also decompose each term in the ray series in such a way so that decomposition into principal and additional components may be facilitated. To perform this task, we need a set of basis vectors aligned along these component directions. Therefore, we can define the following: $\hat{n}^{\nu}_{P}$ is aligned parallel to the tangent vector of the νth ray ($\nu = 0, 1, 2, 3, 4$); $\hat{n}^{\nu}_{SV}$ is a unit vector in the plane of incidence, normal to $\hat{n}^{\nu}_{P}$, and its positive direction is such that $\hat{n}^{\nu}_{SV}\cdot\hat{d}_1 \geq 0$; and, $\hat{n}^{\nu}_{SH}$ is equivalent to the unit vector $\hat{d}_2$. If each term in the ray series expansion is written as

$$\vec{W}^{\nu}_{k} = W^{\nu}_{kP}\hat{n}^{\nu}_{P} + W^{\nu}_{kSV}\hat{n}^{\nu}_{SV} + W^{\nu}_{kSH}\hat{n}^{\nu}_{SH} \tag{2.77}$$

then identification of the principal and additional component for each ray is simple. Of the twelve components associated with the four rays divergent from the boundary, the six principal components are W^1_{kP}, W^2_{kSV}, W^2_{kSH}, W^3_{kP}, W^4_{kSV}, and W^4_{kSH} while the six additional components are W^1_{kSV}, W^1_{kSH}, W^2_{kP}, W^3_{kSV}, W^3_{kSH}, and W^4_{kP} for each value of k. We have dropped the vector notation from these components as the direction of displacement is implied by their subscripts.

Insertion of the ray series, 2.59 and 2.60, into the displacement boundary conditions, 2.70-2.75 yields the following six equations:

$$\sum_{k=0}^{\infty}\left[(-1)^{\epsilon_o}W^o_{k(1)}\right]f_k = \sum_{k=0}^{\infty}\Big[W^1_{kP}\sin\theta_1 + W^1_{kSV}\cos\theta_1 + W^2_{kSV}\cos\theta_2 + W^2_{kP}\sin\theta_2 - W^3_{kP}\sin\theta_3 - W^3_{kSV}\cos\theta_3 - W^4_{kSV}\cos\theta_4 - W^4_{kP}\sin\theta_4\Big]f_k, \tag{2.78}$$

$$\sum_{k=0}^{\infty}\left[(-1)^{\epsilon_o}W^o_{k(2)}\right]f_k = \sum_{k=0}^{\infty}\left[W^1_{kSH} + W^2_{kSH} - W^3_{kSH} - W^4_{kSH}\right]f_k, \tag{2.79}$$

$$\sum_{k=0}^{\infty}\left[(-1)^{\epsilon_o}W^o_{k(n)}\right]f_k = \sum_{k=0}^{\infty}\Big[W^1_{kP}\cos\theta_1 - W^1_{kSV}\sin\theta_1 - W^2_{kSV}\sin\theta_2 + W^2_{kP}\cos\theta_2 + W^3_{kP}\cos\theta_3 - W^3_{kSV}\sin\theta_3 - W^4_{kSV}\sin\theta_4 + W^4_{kP}\cos\theta_4\Big]f_k, \tag{2.80}$$

$$\sum_{k=0}^{\infty}(-1)^{\epsilon_o+1}\left\{-\left[\left(\frac{\lambda_{\epsilon_o}+2\mu_{\epsilon_o}\cos^2\theta_o}{v_o}\right)W^o_{kP} - \mu_{\epsilon_o}\frac{\sin 2\theta_o}{v_o}W^o_{kSV}\right] + \left[\lambda_{\epsilon_o}\vec{\nabla}\cdot\vec{W}^o_{k-1} + 2\mu_{\epsilon_o}W^o_{k-1(n),2}\right]\right\}f_k =$$

$$\sum_{k=0}^{\infty}\left(\sum_{\nu=1}^{4}(-1)^{\epsilon_\nu}\left\{-\left[\left(\frac{\lambda_{\epsilon_\nu}+2\mu_{\epsilon_\nu}\cos^2\theta_\nu}{v_\nu}\right)W^\nu_{kP} - \mu_{\epsilon_\nu}\frac{\sin 2\theta_\nu}{v_\nu}W^\nu_{kSV}\right] + \left[\lambda_{\epsilon_\nu}\vec{\nabla}\cdot\vec{W}^\nu_{k-1} + 2\mu_{\epsilon_\nu}W^\nu_{k-1(n),2}\right]\right\}\right)f_k, \tag{2.81}$$

$$\sum_{k=0}^{\infty}\mu_{\epsilon_o}\left[W^o_{kP}\frac{\sin 2\theta_o}{v_o} + W^o_{kSV}\frac{\cos 2\theta_o}{v_o} - (-1)^{\epsilon_o}\left(W^o_{k-1(1),n} + W^o_{k-1(n),1}\right)\right]f_k =$$

$$\sum_{k=0}^{\infty}\left\{\sum_{\nu=1}^{4}\mu_{\epsilon_\nu}\left[-W^{\nu}_{kP}\frac{\sin 2\theta_\nu}{v_\nu}-W^{\nu}_{kSV}\frac{\cos 2\theta_\nu}{v_\nu}+\right.\right.$$
$$\left.\left.(-1)^{\epsilon_\nu}\left(+W^{\nu}_{k-1(1),n}+W^{\nu}_{k-1(n),1}\right)\right]\right\}f_k, \text{ and} \tag{2.82}$$

$$\sum_{k=0}^{\infty}\mu_{\epsilon_o}\left[W^{o}_{kSH}\frac{\cos\theta_o}{v_o}-(-1)^{\epsilon_o}\left(W^{o}_{k-1(2),n}+W^{o}_{k-1(n),2}\right)\right]f_k =$$
$$\sum_{k=0}^{\infty}\left\{\sum_{\nu=1}^{4}\mu_{\epsilon_\nu}\left[-W^{\nu}_{kSH}\frac{\cos\theta_\nu}{v_\nu}+(-1)^{\epsilon_\nu}\left(W^{\nu}_{k-1(2),n}+W^{\nu}_{k-1(n),2}\right)\right]\right\}f_k. \tag{2.83}$$

Each of the above equations, 2.78 to 2.83 involve a summation over all values of k ($0 \leq k < \infty$) in which a term of the form f_k is always present. For each value of k, we can equate corresponding terms in the summation over both sides of the equation. This property allows us to reduce a problem involving infinite unknowns to an infinite set of systems of equations each involving six equations and six unknowns — the principle components of the generated waves. This system is given as:

$$F_1 = \sin\theta_1 W^1_{kP}+\cos\theta_2 W^2_{kSV}-\sin\theta_3 W^3_{kP}-\cos\theta_4 W^4_{kSV}, \tag{2.84}$$

$$F_2 = \cos\theta_1 W^1_{kP}-\sin\theta_2 W^2_{kSV}+\cos\theta_3 W^3_{kP}-\sin\theta_4 W^4_{kSV}, \tag{2.85}$$

$$F_3 = \rho_1\alpha_1\cos 2\theta_2 W^1_{kP}-\rho_1\beta_1\sin 2\theta_2 W^2_{kSV}-\rho_2\alpha_2\cos 2\theta_4 W^3_{kP}$$
$$+\rho_2\alpha_2\sin 2\theta_4 W^4_{kSV}, \tag{2.86}$$

$$F_4 = \rho_1\gamma_1\beta_1\sin 2\theta_1 W^1_{kP}+\rho_1\beta_1\cos 2\theta_2 W^2_{kSV}+\rho_2\beta_2\gamma_2\sin 2\theta_3 W^3_{kP},$$
$$+\rho_2\beta_2\cos 2\theta_4 W^4_{kSV} \tag{2.87}$$

$$F_5 = W^2_{kSH}-W^4_{kSH}, \text{ and} \tag{2.88}$$

$$F_6 = \rho_1\beta_1\cos 2\theta_2 W^2_{kSH}+\rho_2\beta_2\cos 2\theta_4 W^4_{kSH} \tag{2.89}$$

where F_i is given as the sum of four terms

$$F_i=\sum_{j=1}^{4}F_{ij} \qquad i=1,2,\ldots,6 \tag{2.90}$$

and the F_{ij}'s are

$$F_{11} = (-1)^{\epsilon_o} W^o_{k(1)}, \tag{2.91}$$

$$F_{12} = F_{22} = F_{52} = 0, \tag{2.92}$$

$$F_{13} = -\cos\theta_1 W^1_{kSV} - \sin\theta_2 W^2_{kP} + \cos\theta_3 W^3_{kSV} + \sin\theta_4 W^4_{kP}, \tag{2.93}$$

$$F_{14} = F_{24} = F_{54} = 0, \tag{2.94}$$

$$F_{21} = (-1)^{\epsilon_o} W^o_{k(n)}, \tag{2.95}$$

$$F_{23} = \sin\theta_1 W^1_{kSV} - \cos\theta_2 W^2_{kP} + \sin\theta_3 W^3_{kSV} - \cos\theta_4 W^4_{kP}, \tag{2.96}$$

$$F_{31} = (-1)^{\epsilon_o} \left(\lambda_{\epsilon_o} \frac{\sin\theta_o}{v_o} W^o_{k(1)} + (-1)^{\epsilon_o} (\lambda_{\epsilon_o} + 2\mu_{\epsilon_o}) W^o_{k(n)} \frac{\cos\theta_o}{v_o} \right), \tag{2.97}$$

$$F_{32} = (-1)^{\epsilon_o + 1} \left(\lambda_{\epsilon_o} \vec{\nabla} \cdot \vec{W}^o_{k-1} + 2\mu_{\epsilon_o} W^o_{k-1(n),n} \right), \tag{2.98}$$

$$\begin{aligned} F_{33} = {} & \rho_1 \beta_1 \gamma_1 \sin 2\theta_1 W^1_{kSV} - \frac{\rho_1}{\beta_1} (\alpha_1^2 - 2\beta_1^2 \sin^2\theta_2) W^2_{kP} \\ & - \rho_2 \beta_2 \gamma_2 \sin 2\theta_3 W^3_{kSV} + \frac{\rho_2}{\beta_2} (\alpha_2^2 - 2\beta_2^2 \sin^2\theta_4) W^4_{kP}, \end{aligned} \tag{2.99}$$

$$F_{34} = \sum_{\nu=1}^{4} (-1)^{\epsilon_\nu + 1} \left(\lambda_{\epsilon_\nu} \vec{\nabla} \cdot \vec{W}^\nu_{k-1} + 2\mu_{\epsilon_\nu} W^\nu_{k-1(n),n} \right), \tag{2.100}$$

$$F_{41} = \mu_{\epsilon_o} \left(W^o_{kSV} \frac{\cos 2\theta_o}{v_o} + W_{kP} \frac{\sin 2\theta_o}{v_o} \right), \tag{2.101}$$

$$F_{42} = (-1)^{\epsilon_o + 1} \mu_{\epsilon_o} \left(W^o_{k-1(1),n} + W^o_{k-1(n),1} \right), \tag{2.102}$$

$$\begin{aligned} F_{43} = {} & -\rho_1 \beta_1 \gamma_1 \cos 2\theta_1 W^1_{kSV} - \rho_1 \beta_1 \sin 2\theta_2 W^2_{kP} \\ & - \rho_2 \beta_2 \gamma_2 \cos 2\theta_3 W^3_{kSV} - \rho_2 \beta_2 \sin 2\theta_4 W^4_{kP}, \end{aligned} \tag{2.103}$$

$$F_{44} = \sum_{\nu=1}^{4} (-1)^{\epsilon_\nu + 1} \mu_{\epsilon_\nu} \left(W^\nu_{k-1(1),n} + W^\nu_{k-1(n),1} \right), \tag{2.104}$$

$$F_{51} = (-1)^{\epsilon_o} W^o_{kSH}, \tag{2.105}$$

$$F_{53} = -W^1_{kSH} + W^3_{kSH}, \tag{2.106}$$

$$F_{61} = \mu_{\epsilon_o} \frac{cos\theta_o}{v_o} W^o_{kSH}, \tag{2.107}$$

$$F_{62} = (-1)^{\epsilon_o + 1} \mu_{\epsilon_o} \left(W^o_{k-1(2),n} + W^o_{k-1(n),2} \right), \tag{2.108}$$

$$F_{63} = -\rho_1 \beta_1 \gamma_1 \cos\theta_1 W^1_{kSH} - \rho_2 \beta_2 \gamma_2 \cos\theta_3 W^3_{kSH}, \text{ and} \tag{2.109}$$

$$F_{64} = \sum_{\nu=1}^{4}(-1)^{\epsilon_\nu+1}\mu_{\epsilon_\nu}\left(W^{\nu}_{k-1(2),n}+W^{\nu}_{k-1(n),2}\right). \tag{2.110}$$

First, we solve the problem of the zeroth order terms of the reflected and transmitted waves knowing only the properties of the zeroth order term of the incident ray. The derivative terms in equations 2.81-2.83 are zero as $\vec{W}^{\nu}_{-1} \equiv 0$ and there are no additional components present. In fact, the boundary conditions for the zeroth order waves are identical to Zoeppritz equations which describe plane wave reflection and transmission and can be found in many textbooks such as Fowler [13] and Telford et al. [30]. When we solve for the kth order terms ($k \neq 0$), additional components are present but they may be expressed in terms of the next lowest order term, which we will have already solved.

CHAPTER 3

Dynamic Ray Tracing

3.1 Geometrical Spreading

The previous chapter was devoted to deriving the kinematic and dynamic properties of seismic waves. Approximate forms for the amplitudes of these phases were derived using ART, but a function J was introduced through equation 2.18 in order to describe amplitude variation due to the divergence of rays. In this chapter, we will devote our discussion to deriving this function in continuously varying media as well as establishing boundary conditions to track how it changes across discontinuities. Most of the discussion parallels work already published, mainly by Červený and Hron [5], so the finer details may be examined in that work. However, the last section of the chapter, devoted to discussing the equivalency of two methods of calculating the change in shape of a wavefront at an interface, is not found in any other work.

The zeroth order amplitude for P and S waves have the form

$$W_o = \sqrt{\frac{\rho_o v_o}{\rho v}} \frac{A_o}{\sqrt{J/J_o}} = \sqrt{\frac{\rho_o v_o}{\rho v}} \frac{A_o}{L} \tag{3.1}$$

where ρ is the density, v is the wave speed, A_o is the amplitude at some reference point, and the subscript o refers to quantities measured at this reference point. The

function L is called the geometrical spreading. L is more commonly discussed in the literature than J as it is conceptually clearer to understand, relating how the amplitudes along a wavefront change due to changes in the wavefront's surface area rather than the Jacobian of a transformation from Cartesian coordinates to ray centered coordinates. In spite of this reason, the discussion will be focussed on the derivation of J rather than L, but realizing that the two functions are rather simply related to one another.

3.2 Evaluation of Geometrical Spreading in a continuously varying medium

In order to develop analytical formulae to track geometrical spreading along a ray, we can look at how the local wavefront curvature, $\mathbf{K}$, is changing. $\mathbf{K}$ is a 2×2 matrix involving the two principle radii of curvature of the surface — the radius of curvature along the direction of greatest curvature and the radius of curvature along the direction of least curvature. The explicit form of a curvature matrix is shown later in equations 3.32 and 3.33. However, some preliminary work needs to be done before we can express the curvature of a wavefront in terms of material properties and then to establish a relationship between $\mathbf{K}$ and J.

Our first task is to develop a set of coordinates along the ray that will facilitate our analysis. When dealing with curves in three dimensions it is natural that one of these coordinates should be the arclength, s. It is also natural to select the other two coordinates, q_1 and q_2, such that they are perpendicular to the arclength. Furthermore, as these coordinates are perpendicular to the ray, the

principle components of the S-wave will be coplanar with them. It would be useful to define these coordinates such that this principle component does not rotate within this plane. If the unit vectors of these coordinates, $\hat{e}_1$ and $\hat{e}_2$ are selected such that

$$\hat{e}_1 = \hat{n}\cos\phi(s) - \hat{b}\sin\phi(s) \tag{3.2}$$

$$\hat{e}_2 = \hat{n}\sin\phi(s) + \hat{b}\cos\phi(s) \text{ and} \tag{3.3}$$

$$\phi(s) = \int_{s_o}^{s} T(s')ds' + \phi(s_o), \tag{3.4}$$

this condition is satisfied. In our definitions, we have used the normal and binormal vectors of the ray, $\hat{n}$ and $\hat{b}$, the torsion of the ray, T, the reference arclength along the ray, s_o, and an arbitrary angle $\phi(s_o)$. An infinitesimal distance, dr may be described in this system as:

$$dr^2 = h^2 ds^2 + dq_1^2 + dq_2^2 \tag{3.5}$$

where h is given as

$$h = 1 - K(q_1\cos\phi + q_2\cos\phi) \tag{3.6}$$

and K is the line curvature of the ray.

Červený and Hron [5] showed that the eikonal equation in these ray-centered coordinates may be written as

$$\vec{\nabla}^2\tau = \frac{1}{v^2} = \frac{1}{h^2}\tau^2{}_{,s} + \tau^2{}_{,1} + \tau^2{}_{,2} \tag{3.7}$$

with the comma denoting partial differentiation in the s, q_1, or q_2 direction as indicated. They also showed that the Taylor expansion of τ away from the ray is

$$\tau(s, q_1, q_2) \approx \tau(s, 0, 0) + \frac{1}{2}\vec{q}^T\mathbf{M}\vec{q} \tag{3.8}$$

where

$$\mathbf{M} = \begin{bmatrix} \left.\frac{\partial^2 \tau}{\partial q_1^2}\right|_{q_1=q_2=0} & \left.\frac{\partial^2 \tau}{\partial q_1 \partial q_2}\right|_{q_1=q_2=0} \\ \left.\frac{\partial^2 \tau}{\partial q_1 \partial q_2}\right|_{q_1=q_2=0} & \left.\frac{\partial^2 \tau}{\partial q_2^2}\right|_{q_1=q_2=0} \end{bmatrix} \text{ and } \vec{\mathbf{q}} = \begin{bmatrix} q_1 \\ q_2 \end{bmatrix}.$$

Using the above two results, they were able to show that the matrix $\mathbf{M}$ varies along the ray according to a Riccatti equation:

$$\frac{d\mathbf{M}}{ds} + v\mathbf{M}^2 = -\frac{1}{v^2}\mathbf{V} \tag{3.9}$$

where

$$\mathbf{V} = \begin{bmatrix} v_{,11} & v_{,12} \\ v_{,12} & v_{,22} \end{bmatrix}. \tag{3.10}$$

Deschamps [10], Lee [25], and James [21] showed that $\mathbf{M} = \frac{1}{v}\mathbf{K}$ making it possible to express equation 3.9 in terms of the curvature matrix of the wavefront as

$$v\frac{d\mathbf{K}}{ds} - v_{,s}\,\mathbf{K} + v\mathbf{K}^2 = -\mathbf{V}. \tag{3.11}$$

The function J entered our analysis last chapter through equation 2.18. By noting that $\tau_{,s}^2 = v^{-2}$, we may write:

$$\vec{\nabla}^2\tau = \frac{\partial}{\partial s}\left(\frac{1}{v}\right) + M_{11} + M_{22} = \frac{1}{J}\frac{d}{ds}\left(\frac{J}{v}\right) \tag{3.12}$$

on the central ray (i.e. where $q_1 = q_2 = 0$) so that J can be solved for as

$$J(\tau) = J(\tau_o)\exp\left(\int_{\tau_o}^{\tau} v^2 \mathrm{tr}(\mathbf{M})d\tau'\right) \tag{3.13}$$

or in terms of the wavefront curvature as

$$J(\tau) = J(\tau_o)\exp\left(\int_{\tau_o}^{\tau} v\,\mathrm{tr}(\mathbf{K})d\tau'\right). \tag{3.14}$$

3.3 Boundary Conditions on the Curvature of a Wavefront

We have seen how the curvature of a wavefront may be calculated through a continuously varying medium. It remains to show how a boundary will affect this matrix. Following the procedure of Červený and Hron [5], we shall start by Taylor expanding the phase function τ at a point on the ray defined by an arclength s_o to a point near the ray at coordinates (s, q_1, q_2). This gives us:

$$\tau(s, q_1, q_2) \approx \tau(s_o, 0, 0) + \frac{1}{v_o}(s - s_o) + \frac{1}{2v_o^2} v_{,s} (s - s_o)^2 + \frac{1}{2}\vec{q}^T \mathbf{M} \vec{q} \tag{3.15}$$

where $v_o = v(s_o)$. However, as we wish to express these coordinates in the local Cartesian coordinates of the boundary, we need to express equation 3.15 in a Cartesian coordinate system. By simply replacing the coordinate s with a coordinate l aligned along the tangent vector of the ray, $\hat{t}$ this transformation is possible as the element $dl = hds$. Figure 3.1 shows a plot of these coordinate systems. In the new coordinates, equation 3.15 becomes

$$\tau(l, q_1, q_2) \approx \tau_o + \frac{l}{v_o} - \frac{q_1 v_{,1} + q_2 v_{,2}}{v_o^2} l - \frac{v_{,s}}{2v_o^2} l^2 + \frac{1}{2}\vec{q}^T \mathbf{M} \vec{q} \tag{3.16}$$

where τ_o, v, $v_{,1}$, $v_{,2}$, $v_{,s}$ and $\mathbf{M}$ are evaluated at $(0, 0, 0)$ and all terms greater than second order are neglected.

Now that the Taylor expansion is expressed in terms of a Cartesian coordinate system, we can transform this expansion into another Cartesian frame, this one defined in terms of the local coordinates of the boundary. Thus, we have a basis (d_1, d_2, n) where d_1 is in the intersection of the tangent plane of the boundary and

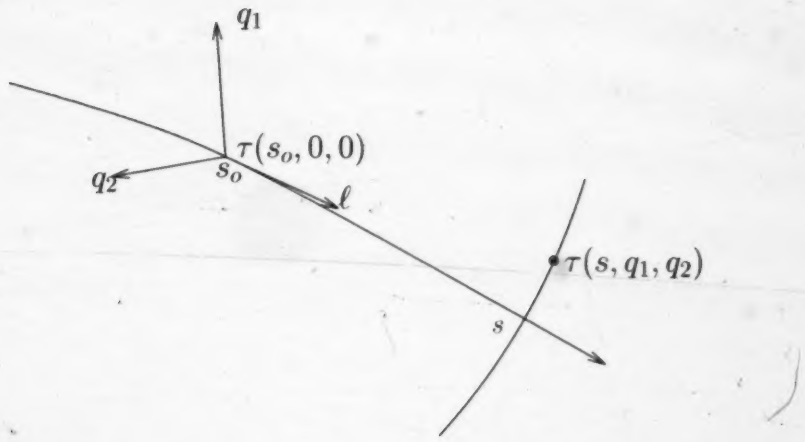

Figure 3.1: A diagram of the (l, q_1, q_2) coordinate system as compared to the (s, q_1, q_2) coordinate system. The point $\tau(s, q_1, q_2)$ may be found from $\tau(s, 0, 0)$ by equation 3.15.

the plane of incidence, d_2 is in the tangent plane of the boundary perpendicular to d_1, and n is in the normal direction of the boundary. Their respective unit vectors, $\hat{d}_1$, $\hat{d}_2$, and $\hat{n}$ are aligned such that $\hat{d}_1 \times \hat{t} > 0$, $\hat{n}$ points into the medium where the ray is coming from, and $\hat{d}_1 \times \hat{d}_2 = \hat{n}$. In our coordinate transformation, we shall simplify the situation by assuming that $\hat{e}_2 = \hat{d}_2$. If only one interface exists along the ray, this assumption amounts to an appropriate choice for ϕ_o but, otherwise, it just serves to simplify the formulae we will derive.

At the boundary, in general, we have five types of waves interacting as discussed in the previous chapter. Physical properties pertinent to the incident ray, such as velocity v and wavefront curvature $\mathbf{K}$, are denoted with the subscript, o while properties pertaining to the reflected or transmitted rays will be given a

subscript, ν. The acute angle between the tangent vector of the ray and $\hat{n}$ is θ. The relationship between the two coordinate systems may then be expressed as:

$$\begin{bmatrix} q_1 \\ q_2 \\ l \end{bmatrix} = \begin{bmatrix} \pm\cos\theta_i & 0 & -\sin\theta_i \\ 0 & 1 & 0 \\ \sin\theta_i & 0 & \pm\cos\theta_i \end{bmatrix} \begin{bmatrix} d_1 \\ d_2 \\ ln \end{bmatrix} \tag{3.17}$$

where the subscript i can be either o or ν and the upper sign corresponds with the reflected waves while the lower sign pertains to the incident and reflected waves. Expressed in these coordinates, the expansion 3.15 becomes

$$\tau(d_1, d_2) \approx \tau_o + \frac{\sin\theta_o}{v} d_1 + \frac{1}{2}\vec{d}^T \mathbf{F} \vec{d} \tag{3.18}$$

where

$$\begin{aligned} \mathbf{F} = & \begin{bmatrix} \pm\cos\theta & 0 \\ 0 & 1 \end{bmatrix} \mathbf{M} \begin{bmatrix} \pm\cos\theta & 0 \\ 0 & 1 \end{bmatrix} \mp \frac{\cos\theta}{v}\mathbf{D} \\ & -\frac{\sin\theta}{v^2} \begin{bmatrix} \pm 2v_{,1}\cos\theta & v_{,2} \\ v_{,2} & 0 \end{bmatrix} - \frac{\sin^2\theta}{v^2} \begin{bmatrix} v_{,s} & 0 \\ 0 & 0 \end{bmatrix}. \end{aligned} \tag{3.19}$$

The expansion is only in two coordinates now as we are considering that the ray is impinging on the surface. The normal vector coordinate was eliminated through the relation

$$n = -\frac{1}{2}\vec{d}^T \mathbf{D} \vec{d} \tag{3.20}$$

which holds locally up to second order accuracy in d_1 and d_2. The vector $\vec{d} = [d_1, d_2]^T$.

Expansions like 3.19 hold for reflected and transmitted waves in the vicinity of the boundary as well as to the incident wave. If we have an expansion for τ for the incident wave and for τ_ν for the reflected or transmitted wave, we have

$$\tau = \tau_\nu. \tag{3.21}$$

Equation 3.21 leads to two conditions. The first is that

$$\frac{\sin\theta_o}{v_o} = \frac{\sin\theta_\nu}{v_\nu} \tag{3.22}$$

which is simply a statement of Snell's Law. The second condition is that

$$\mathbf{F}_o = \mathbf{F}_\nu \tag{3.23}$$

which may be rearranged in terms of curvature matrices to read

$$\mathbf{K}_\nu = \frac{v_\nu}{v_o}\mathbf{S}\mathbf{K}_o\mathbf{S} + v_\nu u\mathbf{G}\mathbf{D}\mathbf{G} + \frac{v_\nu}{v_o}\sin\theta_o\mathbf{G}\mathbf{E}\mathbf{G} \tag{3.24}$$

where **S**, **G**, **E**, and u are defined as follows:

$$\mathbf{S} = \begin{bmatrix} \mp\frac{\cos\theta_o}{\cos\theta_\nu} & 0 \\ 0 & 1 \end{bmatrix},$$

$$\mathbf{G} = \begin{bmatrix} \pm\frac{1}{\cos\theta_\nu} & 0 \\ 0 & 1 \end{bmatrix},$$

$$\mathbf{E} = \begin{bmatrix} 2\left(\frac{v_{o,1}}{v_o}\cos\theta_o \pm \frac{v_{\nu,1}}{v_\nu}\cos\theta_\nu\right) - \frac{\sin\theta_o}{v_o}\left(v_{o,s} - v_{\nu,s}\right) & -\frac{v_{o,2}}{v_o} + \frac{v_{\nu,2}}{v_\nu} \\ -\frac{v_{o,2}}{v_o} + \frac{v_{\nu,2}}{v_\nu} & 0 \end{bmatrix}, \text{ and}$$

$$u = \frac{\cos\theta_o}{v_o} \pm \frac{\cos\theta_\nu}{v_\nu}.$$

Now, we can see that the curvature of the outgoing wavefront is the summation of three terms: one involving the curvature of the incident wavefront; the next involving the curvature of the boundary; and finally a term related to velocity gradients near the boundary.

Finally, we can derive the formula for the change in wavefront curvature at a boundary neglecting the assumption that $\hat{q}_2 \cdot \hat{x}_2 = 1$ but instead proceeding to the most general case where the two unit vectors are separated by an angle $\Omega = \cos^{-1}(\hat{q}_2 \cdot \hat{x}_2)$. The curvature of the outgoing wavefront is then given as

$$\mathbf{K}_\nu = \frac{v_\nu}{v_o}\mathbf{S}\mathbf{W}^T\mathbf{K}_o\mathbf{W}\mathbf{S} + v_\nu u\mathbf{G}\mathbf{D}\mathbf{G} + \frac{v_\nu}{v_o}\sin\theta_o\mathbf{G}\overline{\mathbf{E}}\mathbf{G} \tag{3.25}$$

where $\mathbf{W}$ is a rotation matrix equal to

$$\mathbf{W} = \begin{bmatrix} \cos\Omega & \sin\Omega \\ -\sin\Omega & \cos\Omega \end{bmatrix} \tag{3.26}$$

and $\overline{\mathbf{E}}$ is equal to the matrix $\mathbf{E}$ replacing $v_{,1}$ with $(v_{,1}\cos\Omega + v_{,2}\sin\Omega)$ and $v_{,2}$ by $(v_{,1}\sin\Omega - v_{,2}\cos\Omega)$.

3.4 Gel'chinskiy's Equations

Another method exists to define the change in wavefront curvature. Derived by Gel'chinskiy [14] from differential geometry, this system gives the relationship in terms of principle radii of curvature in contrast to equation 3.24 which gives the solution in terms of the 2×2 curvature matrix as the summation of three matrix terms. However, by starting with equation 3.24 and deriving Gel'chinskiy's equations, we will show that these two systems are equivalent.

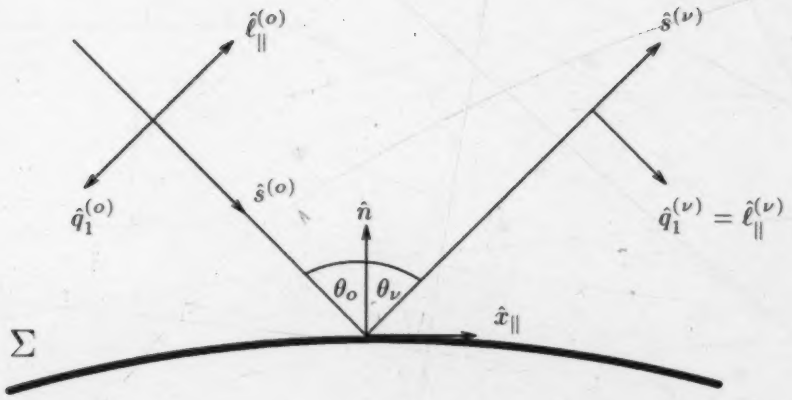

Figure 3.2: The unit vectors for the ray centered coordinate system and Gel'chinskiy's equations for an incident and a reflected ray near a boundary Σ in the plane of incidence.

Gel'chinskiy's formulae use coordinates aligned in the tangent planes of the wavefront, $\hat{\ell}_{\|}$, and the boundary, $\hat{x}_{\|}$ and $\hat{x}_{\perp}$. The vectors with the $\|$ subscript are aligned parallel to the plane of incidence while $\hat{x}_{\perp}$ is perpendicular to this plane. In addition, the positive direction of $\hat{x}_{\|}$ is such that the component of the incident ray parallel to $\hat{x}_{\|}$ is positive, $\hat{x}_{\|} \cdot \hat{\ell}_{\|}$ is positive, and $\hat{x}_{\|} \times \hat{x}_{\perp} = \hat{n}$.

Gelchinskiy's [14] equations to describe the radii of curvature of an outgoing wavefront, $r_1^{(\nu)}$ and $r_2^{(\nu)}$, as a function of the radii of curvature of the incoming wavefront, $r_1^{(o)}$ and $r_2^{(o)}$, the radii of curvature of the boundary, R_1 and R_2, and the velocity distribution along the boundary have the form:

$$\frac{1}{r_1^{(\nu)}}, \frac{1}{r_2^{(\nu)}} = \frac{1}{2}\left[A + B \pm \frac{\sqrt{(A-B)^2\cos^2\theta_\nu + 4C^2}}{\cos\theta_\nu}\right] \text{ and} \tag{3.27}$$

$$\phi_\nu = \frac{1}{2}\tan^{-1}\left[\frac{2C}{(A-B)\cos\theta_\nu}\right] \tag{3.28}$$

where

$$\begin{aligned} A &= \frac{1}{\cos\theta_\nu}\left[-\sin\theta_o\frac{\partial v_\nu}{\partial \ell_{\|}^{(\nu)}} + \left(\sin\theta_o\frac{\partial}{\partial x_{\|}}\left(\frac{v_\nu}{v_o}\right) - \frac{v_\nu}{v_o}\frac{\sin 2\theta_o}{2v_o}\frac{\partial v_o}{\partial \ell_{\|}^{(o)}}\right)\right] \\ &\quad + \frac{1}{\cos^2\theta_\nu}\left[\frac{v_\nu}{v_o}\frac{\cos^2\theta_o}{r_{\|}^{(o)}} + \frac{(v_\nu/v_o)\cos\theta_o \pm \cos\theta_\nu}{R_{\|}}\right], \end{aligned} \tag{3.29}$$

$$B = \frac{v_\nu}{v_o}\frac{1}{r_\perp^{(o)}} + \frac{(v_\nu/v_o)\cos\theta_o \pm \cos\theta_\nu}{R_\perp}, \text{ and} \tag{3.30}$$

$$\begin{aligned} C &= -\frac{v_\nu}{v_o}\cos\theta_o\frac{\sin 2\phi_o}{2}\left(\frac{1}{r_1^{(o)}} - \frac{1}{r_2^{(o)}}\right) + \sin\theta_o\frac{\partial}{\partial x_{\|}}\left(\frac{v_\nu}{v_o}\right) \\ &\quad + \frac{\sin 2\psi}{2}\left(\frac{1}{R_1} - \frac{1}{R_2}\right)\left(\frac{v_\nu}{v_o}\cos\theta_o \pm \cos\theta_\nu\right). \end{aligned} \tag{3.31}$$

In the above equations, ϕ_ν, ϕ_o, and ψ are the angles at which the the first principle normal section of the scattered wavefront, incident wavefront, and boundary, respectively, are rotated with respect to the plane of incidence. Also, the $\|$ and $\perp$ subscripts refer to the radii of curvature measured in the plane parallel (in the former case) and perpendicular (in the latter case) to the plane of incidence and may be determined from known quantities, as shown later in equations 3.34 and 3.35. The radii of curvature of the boundary are positive if the boundary is seen as convex from the medium containing the incident wave. It must be noted that, with the exception of equation 3.27 and later equation 3.48, the upper sign in all formulae in this section refers to upgoing waves while the lower sign refers to downgoing waves.

In general, the curvature matrix, $\mathbf{K}'$, of a regular surface may be described in terms of its principle radii of curvature, ρ_1 and ρ_2. In a reference frame aligned such that these radii of curvature are along the axes of the frame, $\mathbf{K}'$ has the following

form:

$$\mathbf{K}' = \begin{bmatrix} \rho_1 & 0 \\ 0 & \rho_2 \end{bmatrix}. \tag{3.32}$$

When this reference frame is rotated by an angle α from these principle radii, $\mathbf{K}'$ becomes

$$\begin{aligned} \mathbf{K}' &= \begin{bmatrix} \cos\alpha & \sin\alpha \\ -\sin\alpha & \cos\alpha \end{bmatrix} \begin{bmatrix} \rho_1 & 0 \\ 0 & \rho_2 \end{bmatrix} \begin{bmatrix} \cos\alpha & -\sin\alpha \\ \sin\alpha & \cos\alpha \end{bmatrix} \\ &= \begin{bmatrix} \frac{\cos^2\alpha}{\rho_1} + \frac{\sin^2\alpha}{\rho_2} & \cos\alpha\sin\alpha\left(\frac{1}{\rho_1} - \frac{1}{\rho_2}\right) \\ \cos\alpha\sin\alpha\left(\frac{1}{\rho_1} - \frac{1}{\rho_2}\right) & \frac{\sin^2\alpha}{\rho_1} + \frac{\cos^2\alpha}{\rho_2} \end{bmatrix}. \end{aligned} \tag{3.33}$$

It is important to note that the Gaussian curvature, $\kappa' = \det(\mathbf{K}')$, and the mean curvature, $H' = 1/2\mathrm{tr}(\mathbf{K}')$ are invariant under this rotation. For the sake of brevity the plane curvature measured along the axes of the rotation plane, from now on referred to as the parallel curvature, $\rho_{\|}$, and perpendicular curvature, $\rho_{\perp}$, are defined as follows:

$$\rho_{\|} = \frac{\cos^2\alpha}{\rho_1} + \frac{\sin^2\alpha}{\rho_2}, \text{ and} \tag{3.34}$$

$$\rho_{\perp} = \frac{\sin^2\alpha}{\rho_1} + \frac{\cos^2\alpha}{\rho_2}. \tag{3.35}$$

To compare the two systems, it is useful to compose each matrix component of equation 3.24 in terms of the radii of curvature of the scattered wavefront. This procedure may be accomplished with the aid of equations 3.33 to 3.35. The diagonal terms in equation 3.24 are:

$$\frac{1}{r_{\|}^{(\nu)}} = \frac{v_\nu}{v_o}\frac{\cos^2\theta_o}{\cos^2\theta_\nu}\frac{1}{r_{\|}^{(o)}} + 2\frac{v_\nu}{v_o}\sin\theta_o\left(\frac{v_{o,1}}{v_o}\frac{\cos\theta_o}{\cos^2\theta_\nu} \pm \frac{v_{\nu,1}}{v_\nu}\frac{1}{\cos\theta_\nu}\right)$$

$$+\frac{1}{\cos^2\theta_\nu}\left(\frac{v_\nu}{v_o}\cos\theta_o \pm \cos\theta_\nu\right)\frac{1}{R_\parallel} - \frac{v_\nu}{v_o^2}\frac{\sin^2\theta_o}{\sin\theta_\nu}(v_{o,s} - v_{\nu,s}) \text{ and} \quad (3.36)$$

$$\frac{1}{r_\perp^{(\nu)}} = \frac{v_\nu}{v_o}\frac{1}{r_\perp^o} + \left(\frac{v_\nu}{v_o}\cos\theta_o \pm \cos\theta_\nu\right)\frac{1}{R_\perp}. \quad (3.37)$$

As curvature matrices are symmetric, the off-diagonal components of $\mathbf{K}_\nu$ in equation 3.24 are identical and equal to

$$\frac{\sin 2\phi_\nu}{2}\left(\frac{1}{r_1^{(\nu)}} - \frac{1}{r_2^{(\nu)}}\right) =$$
$$\pm\left[\frac{1}{\cos\theta_\nu}\left(\frac{v_\nu}{v_o}\cos\theta_o \pm \cos\theta_\nu\right)\left(\frac{1}{R_1} - \frac{1}{R_2}\right)\frac{\sin 2\psi}{2}\right.$$
$$\left. - \frac{v_\nu}{v_o}\frac{\cos\theta_o}{\cos\theta_\nu}\left(\frac{1}{r_1^{(o)}} - \frac{1}{r_2^{(o)}}\right)\frac{\sin 2\phi_o}{2} \pm \frac{v_\nu}{v_o}\frac{\sin\theta_o}{\cos\theta_\nu}\left(\frac{v_{\nu,2}}{v_\nu} - \frac{v_{o,2}}{v_o}\right)\right]. \quad (3.38)$$

It is evident from equation 3.37 that

$$\frac{1}{r_\perp^{(\nu)}} = B. \quad (3.39)$$

Equations 3.36 and 3.38 may also be related to the A and C terms in Gel'chinskiy's equations. However, since these equations contain directional derivatives in different coordinate systems, these need to be related to one another. Thus:

$$v_{,1} = \pm\frac{\partial v}{\partial \ell_\parallel}, \quad (3.40)$$

$$v_{,2} = \frac{\partial v}{\partial x_\perp}, \text{ and} \quad (3.41)$$

$$v_{,s} = \vec{\nabla} v \cdot \hat{s} = \vec{\nabla} v \cdot \left(\frac{1}{\sin\theta}\hat{x_\parallel} - \frac{\cos\theta}{\sin\theta}\hat{\ell_\parallel}\right)$$
$$= \frac{1}{\sin\theta}\frac{\partial v}{\partial x_\parallel} - \frac{\cos\theta}{\sin\theta}\frac{\partial v}{\partial \ell_\parallel}. \quad (3.42)$$

Substitution of these terms into equations 3.36 and 3.37 yields:

$$\frac{1}{r_\parallel^{(\nu)}} = A \text{ and} \quad (3.43)$$

$$\frac{\sin 2\phi_\nu}{2}\left(\frac{1}{r_1^{(\nu)}}-\frac{1}{r_2^{(\nu)}}\right)=\frac{\pm C}{\cos\theta_\nu}. \tag{3.44}$$

Therefore, the curvature matrix of the outgoing wavefront has the form:

$$\mathbf{K}_\nu=\begin{bmatrix} A & \frac{\pm C}{\cos\theta_\nu} \\ \frac{\pm C}{\cos\theta_\nu} & B \end{bmatrix}. \tag{3.45}$$

The mean curvature, H, and the Gaussian curvature, κ of this surface are expressed as follows:

$$H = \frac{1}{2}\mathrm{tr}(\mathbf{K}_\nu)=\frac{A+B}{2} \text{ and} \tag{3.46}$$

$$\kappa = \det(\mathbf{K}_\nu)=AB-\frac{C^2}{\cos^2\theta_\nu}. \tag{3.47}$$

Knowing these two quantities, the principle radii of curvature may be determined as the inverses of the roots of a quadratic equation:

$$\frac{1}{r_1^{(\nu)}},\frac{1}{r_2^{(\nu)}}=H\pm\sqrt{H^2-\kappa}=\frac{1}{2}\left[A+B\pm\frac{\sqrt{(A-B)^2\cos^2\theta_\nu+4C^2}}{\cos\theta_\nu}\right]. \tag{3.48}$$

To get the value of ϕ_ν one first has to use the result of equation 3.48 to substitute the values of the principle radii of curvature into equation 3.44 to obtain:

$$\frac{\sin 2\phi_\nu}{2}\left(\frac{1}{r_1^{(\nu)}}-\frac{1}{r_2^{(\nu)}}\right)=\frac{\sin 2\phi_\nu}{2}\left[\frac{\sqrt{(A-B)^2\cos^2\theta_\nu+4C^2}}{\cos\theta_\nu}\right]=\frac{\pm C}{\cos\theta_\nu} \tag{3.49}$$

which may solved for ϕ_ν as

$$\phi_\nu=\tan^{-1}\left[\frac{2C}{(A-B)\cos\theta_\nu}\right]. \tag{3.50}$$

Clearly, the matrix system of equations developed by Červený and Hron may be reduced to Gel'chinskiy's result and the two methods for evaluating the shape of transmitted and reflected wavefronts are equivalent.

CHAPTER 4

Modelling the Effect of Velocity Gradients in the Change in Geometrical Spreading Across a Boundary

4.1 Introduction

Traditional views of the focussing of seismic energy at a boundary only stress the influence of boundary curvature. For example, several authors, such as Deschamps [10], Lee [25], and James [21], detail the effect of boundary curvature on the curvature of electromagnetic wavefronts. No attention was paid to the effect of velocity gradients near the boundaries. However, as we have seen in the previous chapter, the Dynamic Ray Tracing system, as developed in Červený and Hron [5], predicts that the curvature of reflected or transmitted wavefronts must also depend on the magnitude and direction of local velocity gradients in the vicinity of the boundary. As wavefront curvature and geometrical spreading are intimately related, local velocity gradients can act to focus and defocus seismic energy. Knowledge of this effect is very important to the study of the Earth as much of the Earth's material contains velocity gradients with depth as shown in the Preliminary Reference Earth Model (PREM) of Dziewonski and Anderson [12] in Figure 4.1.

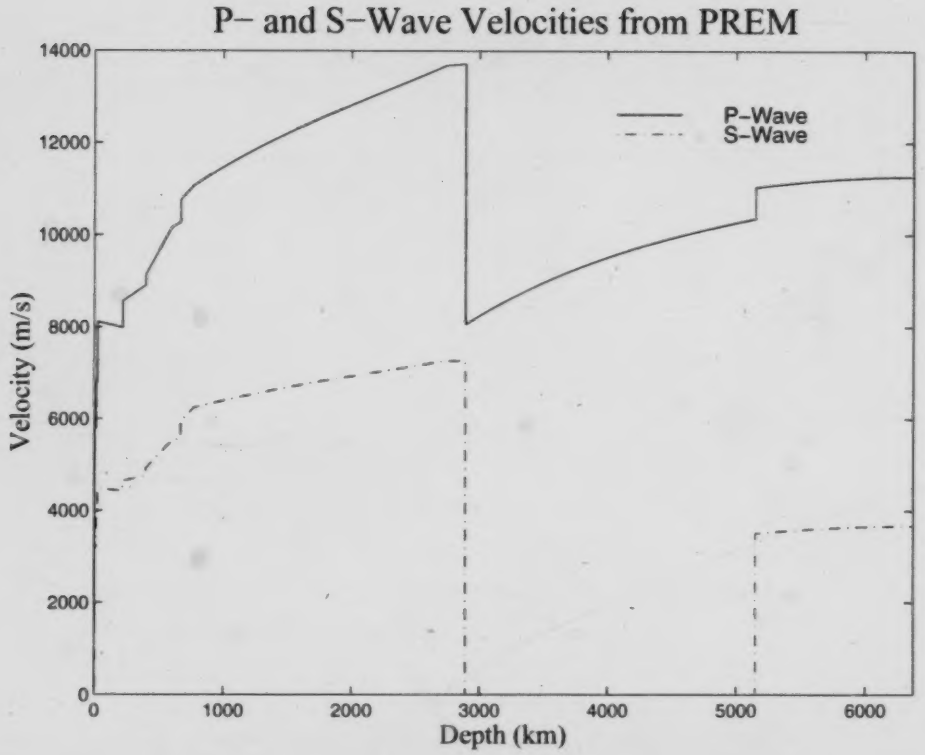

Figure 4.1: Velocities from PREM of Dziewonski and Anderson [12]. The velocity profile for P- and S- waves contain discontinuities with gradients on either side.

4.2 Ray Tracing in a Constant Gradient Medium

As we will be considering the special case of a wave propagating through media with constant velocity gradients, we can arrive at analytical expressions to describe both the ray path and the geometrical spreading term anywhere on the ray. This problem, with respect to arc length along the ray, was first considered by Hubral [20] but we will be following a derivation describing the results with respect to traveltime instead.

4.2.1 Ray Paths

The velocity in a medium can be described by three parameters if the gradient is constant: we need the value of velocity at one point, v_o; the magnitude of the velocity gradient, $|\vec{\nabla} v|$, is required; and the direction of the velocity gradient, ϕ, is also needed. Nettleton [28] showed that a ray path in such a medium follows the arc of a circle whose center and radius are functions of these parameters together with the take-off angle relative to the direction of the velocity gradient, θ_o.

We shall assume that a two dimensional reference coordinate system (x, z), as shown in figure 4.2, is used to describe a point in a medium. At the origin (which corresponds to the point at which a ray enters the medium via, either a source, a reflection, or a transmission) the velocity is given as v_o. There also exists a velocity gradient, $\vec{\nabla} v$, parallel to a coordinate axis, z', which is rotated from the z-axis by an angle, ϕ such that $-\frac{\pi}{2} \leq \phi \leq \frac{\pi}{2}$. In this way, the projection of $\vec{\nabla} v$ on the z'-axis may be given a scalar value, g, which can be either positive or negative. If we define a x'-axis, perpendicular to the z'-axis, we can define the rotation of coordinates from

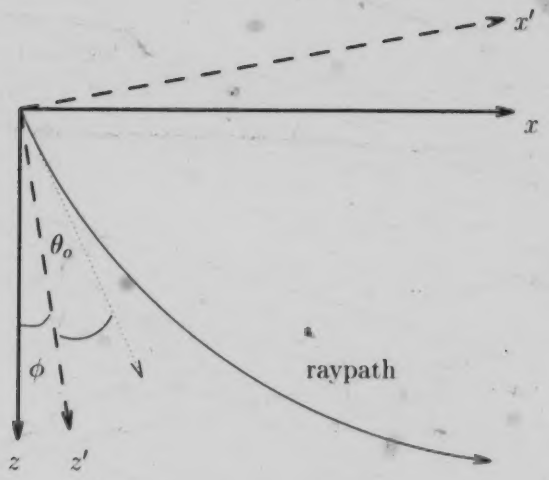

Figure 4.2: The coordinate systems used for a ray propagating in a medium with a constant gradient.

the reference (x, z) system as

$$\begin{bmatrix} x' \\ z' \end{bmatrix} = \begin{bmatrix} \cos\phi & \sin\phi \\ -\sin\phi & \cos\phi \end{bmatrix} \begin{bmatrix} x \\ z \end{bmatrix}. \tag{4.1}$$

In figure 4.2, the positive direction of ϕ is given in the counter-clockwise direction.

The coordinate rotation is necessary so that we can compare our model with the scenario considered by Nettleton [28] of a velocity field described by

$$v(z') = v_o + gz'. \tag{4.2}$$

The ray path is contained in the (x', z') plane and follows an arc of the circle described by

$$\left(x' - \frac{v_o \cot\theta_o}{g}\right)^2 + \left(z' + \frac{v_o}{g}\right)^2 = \left(\frac{v_o}{g\sin\theta_o}\right)^2. \tag{4.3}$$

To glean more information about the ray, we must use the characteristic equations of the ray

$$\frac{dx'}{d\tau} = v(z')\sin\theta(\tau), \tag{4.4}$$

$$\frac{dz'}{d\tau} = v(z')\cos\theta(\tau), \text{ and} \tag{4.5}$$

$$\frac{d\theta}{d\tau} = \frac{dv}{dz'}\sin\theta(\tau) \tag{4.6}$$

where τ is the traveltime along the ray, v is the velocity of the ray, and $\theta(\tau)$ is the acute angle between the ray and the z'-axis. Integration of these equations, 4.4-4.6, yields the following equations as given by Marks [26]:

$$x'(\tau) = \frac{v_o}{g}\tan\frac{\theta_o}{2}\frac{e^{2g\Delta\tau} - 1}{1 + Ae^{2g\Delta\tau}}, \tag{4.7}$$

$$z'(\tau) = \frac{v_o}{g}\left[\frac{(1+A)e^{g\Delta\tau}}{1 + Ae^{2g\Delta\tau}} - 1\right], \tag{4.8}$$

$$\theta(\tau) = 2\tan^{-1}\left[e^{g\Delta\tau}\tan\left(\frac{\theta_o}{2}\right)\right], \tag{4.9}$$

$$v(\tau) = v_o\frac{(1+A)e^{g\Delta\tau}}{1 + Ae^{2g\Delta\tau}}, \text{ and} \tag{4.10}$$

$$\Delta\tau = \tau - \tau_o = \frac{1}{|g|}\cosh^{-1}\left[\frac{g^2(x'^2 + z'^2)}{2v(\tau)v_o} + 1\right] \tag{4.11}$$

where τ_o is the traveltime at the origin and $A = \tan^2\frac{\theta_o}{2}$.

We now have all the tools necessary to find the path of a ray through a constant gradient medium. For the case that we will be examining, we can determine

the incident point of a ray on a plane boundary by finding the intersection of a circle and a line in the (x', z') plane with the use of equation 4.3. Though this gives us two roots in general, the root closest to the source is the point of incidence. If no real solution exists, the ray is a diving ray and it turns before encountering the boundary.

4.2.2 Geometrical Spreading

We can now turn our attention to how amplitude varies along the ray in a constant gradient medium. For the zeroth order amplitude terms in ART, the amplitudes are controlled by two factors if the source is isotropic: the ratio of acoustic impedances between the source and the observation point can be well determined as we know the elastic parameters everywhere in the medium; on the other hand, derivation of the relative geometrical spreading term in such a medium, L_i, requires that we examine the Riccati equation in $\mathbf{M}$, 3.9, the matrix of spatial phase derivatives from DRT. In this type of medium, the equation is simplified appreciably as the matrix of the second derivatives of the velocity field, $\mathbf{V} = \mathbf{0}$, and we have the freedom to align the ray centered coordinates such that

$$\mathbf{M} = \begin{bmatrix} M_{11} & 0 \\ 0 & M_{22} \end{bmatrix}. \tag{4.12}$$

Abandoning the matrix notation we have

$$\frac{dM_{11}}{d\tau} + v^2 M_{11}^2 = 0 \text{ and} \tag{4.13}$$

$$\frac{dM_{22}}{d\tau} + v^2 M_{22}^2 = 0. \tag{4.14}$$

The Jacobian of the transformation from Cartesian coordinates to ray coordinates, J, may be expressed in terms of the matrix components of $\mathbf{M}$ by equation 3.13. We can define the relative geometrical spreading through the medium, L_i, by

$$L_i(\tau) = \sqrt{\frac{J(\tau)}{J(\tau_i)}} = \exp\left[\frac{1}{2}\int_{\tau_i}^{\tau} v^2(M_{11} + M_{22})d\tau'\right]. \tag{4.15}$$

where τ_i is the traveltime to the ith interface along the ray and the ray does not encounter any other interfaces from τ_i up to the travetime τ. We will find it convenient to express L_i as the product of a geometrical spreading term in the (x', z') plane,

$$L_{i\parallel} = \exp\left[\frac{1}{2}\int_{\tau_i}^{\tau} v^2 M_{11} d\tau'\right] = \left(\frac{v(\tau)r_{\parallel}(\tau)}{v(\tau_i)r_{\parallel}(\tau_i)}\right)^{\frac{1}{2}} \tag{4.16}$$

and a similar term in the rectifying plane of the ray (defined to contain the ray's tangent vector and binormal vector):

$$L_{i\perp} = \exp\left[\frac{1}{2}\int_{\tau_i}^{\tau} v^2 M_{22} d\tau'\right] = \left(\frac{v(\tau)r_{\perp}(\tau)}{v(\tau_i)r_{\perp}(\tau_i)}\right)^{\frac{1}{2}} \tag{4.17}$$

where $r_{\parallel}$ and $r_{\perp}$ are the radii of curvature of the wavefront in the (x', z') and the rectifying planes respectively. The only unknowns in equations 4.16 and 4.17 are $r_{\parallel}(\tau)$ and $r_{\perp}(\tau)$. We need to return to equations 4.13 and 4.14 in order to determine these quantities. Due to the symmetries in equations 4.13 and 4.14, we will examine only equation 4.13 as the development of equation 4.14 will be redundant. Integration of equation 4.13 yields:

$$\frac{1}{M_{11}(\tau)} - \frac{1}{M_{11}(\tau_i)} = \int_{\tau_i}^{\tau} v^2(\tau')d\tau'. \tag{4.18}$$

By noting that $M_{11}(\tau) = \frac{1}{v(\tau)r_{\|}(\tau)}$ equation 4.18 may be solved for $r_{\|}$. Thus,

$$r_{\|}(\tau) = \frac{v(\tau_i)}{v(\tau)} r_{\|}(\tau_i) + \frac{1}{v(\tau)} \int_{\tau_i}^{\tau} v^2(\tau') d\tau'. \tag{4.19}$$

Using equation 4.10, the integral in equation 4.19 may be evaluated to give

$$\int_{\tau_i}^{\tau} v^2(\tau') d\tau' = \frac{v(\tau_i)v(\tau)}{g} \sinh(g\Delta\tau) = v(\tau_i)\Delta r \tag{4.20}$$

where $\Delta r = \frac{v(\tau)}{g} \sinh(g\Delta\tau)$ describes the amount of change in the radii of curvature of the wavefront. The geometrical spreading term, L_i, may be expressed as the product of a contribution from the change in curvature in the (x', z') plane, $L_{\|}$, and a similar contribution perpendicular to this plane, $L_{\perp}$. The $L_{\|}$ and $L_{\perp}$ terms are

$$L_{i\|}(\tau) = \sqrt{\frac{r_{\|}(\tau_i) + \Delta r}{r_{\|}(\tau_i)}} \text{ and} \tag{4.21}$$

$$L_{i\perp}(\tau) = \sqrt{\frac{r_{\perp}(\tau_i) + \Delta r}{r_{\perp}(\tau_i)}}. \tag{4.22}$$

The quantity, $L_i = L_{i\|} L_{i\perp}$, which we have called geometrical spreading in this derivation, is only the measure of how the total geometrical spreading, L, varies along the ith segment of the ray. If there exist any boundaries between the source and the observation point along the ray, then these quantities are unequal. The geometrical spreading of a ray travelling though n layers is given as

$$L = \prod_{i=1}^{n} L_i. \tag{4.23}$$

The radii of curvature of the wavefront at the entry point of a ray into a medium may be determined through the properties of the incident wavefront by equation 3.24. The only problem remains in dealing with the first segment of the ray travelling form

the source. A wavefront from a point source has infinite curvature at traveltime, $\tau_o = 0$. Substitution of $\tau_o = 0$ into equations 4.21 and 4.22 yields infinite geometrical spreading. In order to circumvent this singularity, the geometrical spreading will only begin to be tracked a finite distance away from the source to a point O_o at a traveltime τ_o' where $r_{\|}(\tau_o') = r_{\perp}(\tau_o') = 1$ in arbitrary units of length. Thus, the geometrical spreading of this first ray segment beyond O_o may be expressed as

$$L_1(\tau) = 1 + \frac{v(\tau)}{g} \sinh[g(\tau - \tau_o')] \tag{4.24}$$

where

$$\tau_o' = \frac{1}{g} \sinh^{-1}\left(\frac{g}{v_o}\right). \tag{4.25}$$

4.3 The Effect of a Boundary

4.3.1 Amplitude Versus Offset Curves for Constant Gradient Media

We will display how velocity gradients may act to focus or defocus seismic rays by running a Gedanken experiment where a point source is exploded isotropically on the surface of a layer over a half space. The two layers are both inhomogeneous, with constant gradients in P-wave and S-wave velocity and a receiver may be buried in the lower medium or on the surface of the upper medium to record the transmitted and reflected wave amplitudes respectively. The boundary between the two media will be a plane so that the curvature of the generated wavefront is a function of only the curvature of the incident wavefront and the velocity gradients. By contrasting the amplitudes derived from inclusion or exclusion of the third term

in equation 3.24, used to describe the change in wavefront curvature at the boundary, we can display how velocity gradients affect the observed amplitudes of these arrivals. The amplitudes we derive will only be the zeroth order term of the ray series expansion.

We have used the following scheme to label the arrivals in the figures in the section. P1P1, P1S1, P1P2, and P1S2 refer to the reflected P-wave, the reflected S-wave, the transmitted P-wave, and the transmitted S-wave respectively. Figure 4.3 shows all of these arrivals. The reflected wave amplitudes are recorded at the surface and therefore surface conversion coefficients are applied while the transmitted waves are recorded at the deepest point in each model by a receiver buried within the underlying medium.

The first model we will consider has two layers after the Mississippi model as found in Choi [8]. The properties of this layer are displayed in figure 4.4. There exists a positive gradient for v_p, v_s, and ρ in the top layer. For the source at zero depth, this gradient produces concave ray paths when viewed from the surface. Figure 4.5 shows the ray paths for a non-phase converted reflection in this model. The gradient also affects the change in geometrical spreading across a boundary, much like the effect of boundary curvature. However, unlike the effect of curvature, the magnitude of the velocity gradient effect is proportional to ray parameter so that large effects will be observed at far offsets and no effect will be seen at zero offset.

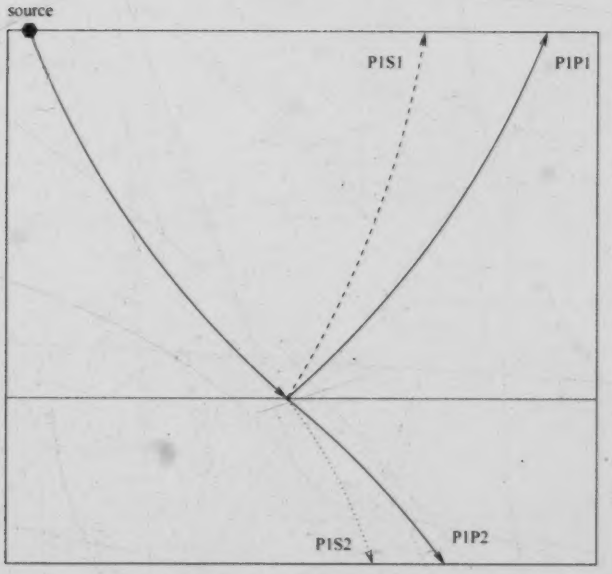

Figure 4.3: A plot of the arrivals examined in this section. The dashed rays denote shear waves and the solid rays denote P-waves.

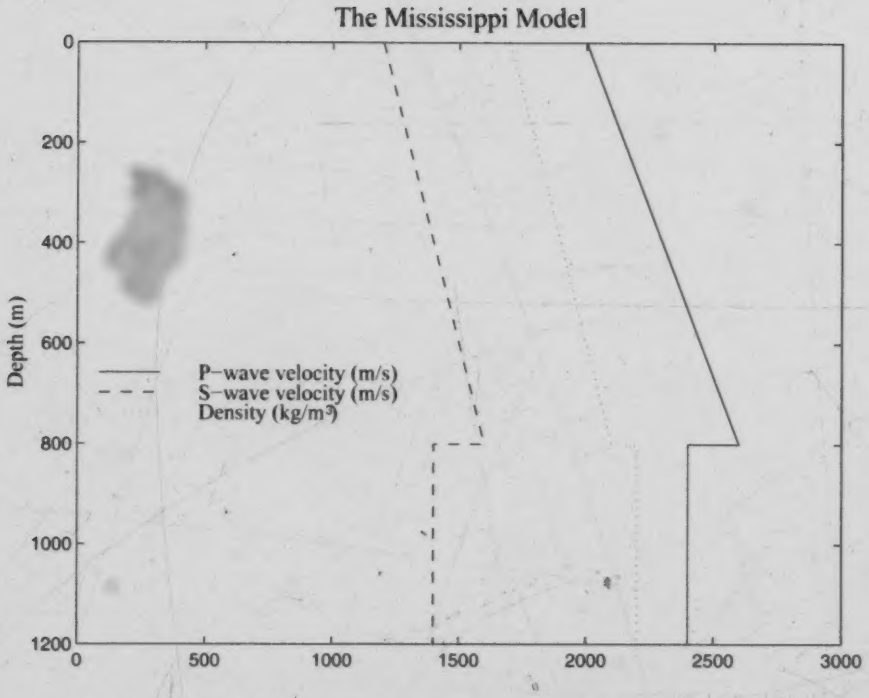

Figure 4.4: The Mississippi Model.

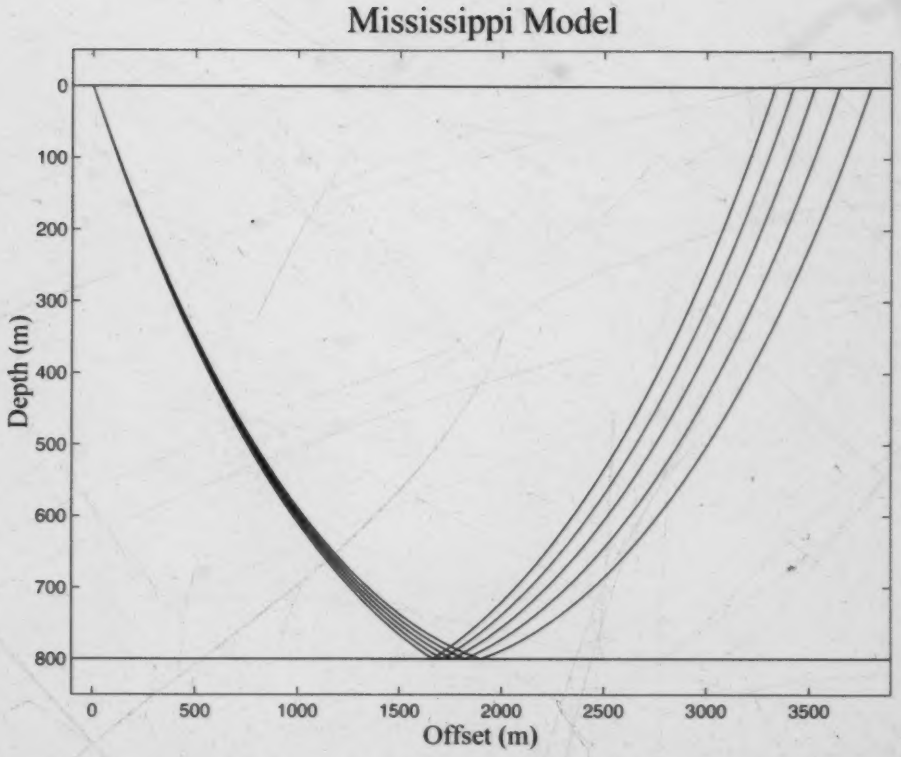

Figure 4.5: Rays for the primary non-phase converted reflection in the Mississippi Model.

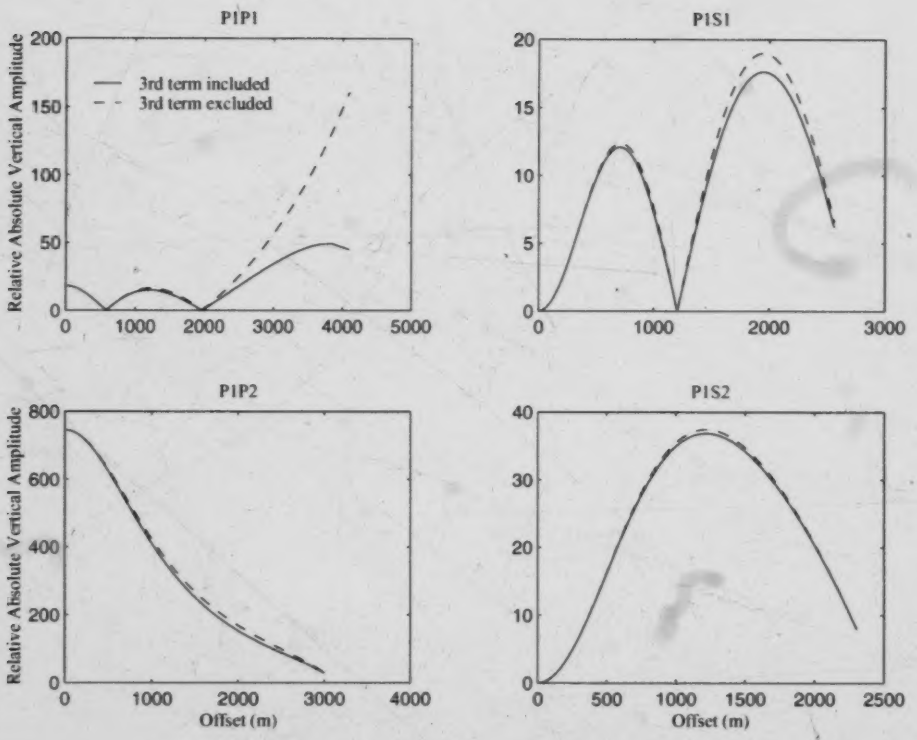

Figure 4.6: The calculated vertical component amplitudes of reflected and transmitted arrivals from an isotropic point source located on the surface of the Mississippi Model recorded at a receiver on the surface. The difference in amplitude of the two curves in each plot is due to inclusion or exclusion of the effects of velocity gradients on the jump in geometrical spreading across the boundary at 800 m.

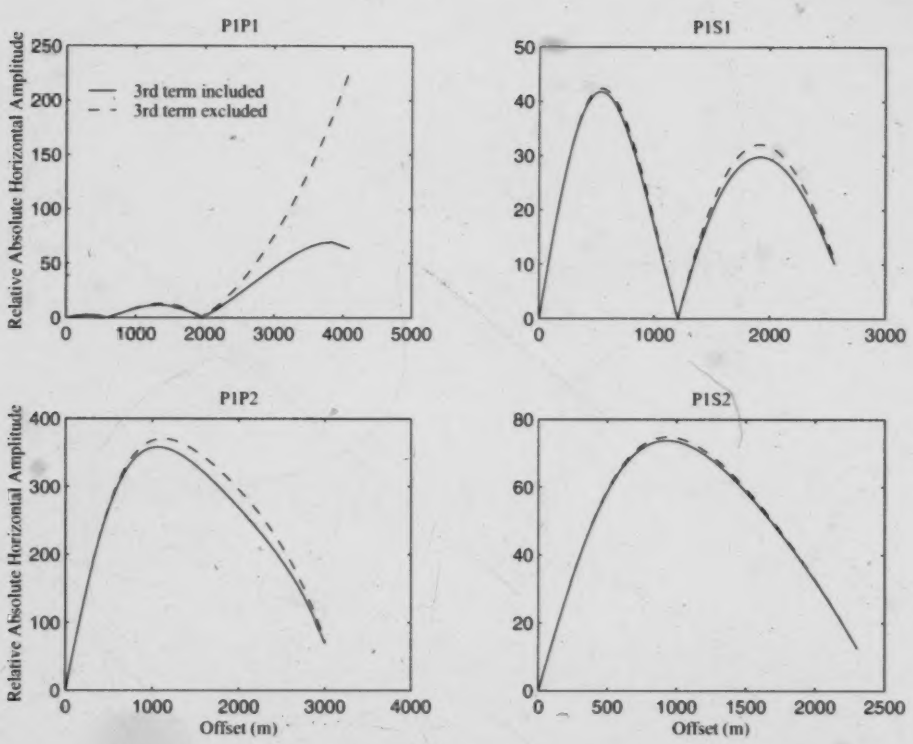

Figure 4.7: The calculated horizontal component amplitudes of reflected and transmitted arrivals from an isotropic point source located on the surface of the Mississippi Model recorded at a receiver on the surface. The difference in amplitude of the two curves in each plot is due to inclusion or exclusion of the effects of velocity gradients on the jump in geometrical spreading across the boundary at 800 m.

When the effect of velocity gradients on the jump in geometrical spreading is ignored by exclusion of the third term in equation 3.24, the amplitude of the primary reflection is greatly increased compared to the real case, where this amplitude is included. This is shown in figures 4.6 and 4.7. The discrepancy between the two curves is greatest at farthest offset which is expected as the velocity gradient term in Červený and Hron's formula, equation 3.24, is dependent on ray parameter. This is the term referred to as the 3rd term in the legend of figure 4.6. For the primary reflection, P1P1, the effect of the velocity gradients is most noticeable though it has influence in all of the other arrivals. The effect is least noticeable in the transmitted arrivals as the 3rd term involves the velocity gradients, which are zero in the lower layer. The positive gradient in the first layer defocusses the seismic energy of a reflected wave. That is, there is less amplitude in the arrivals.

It is important to note, the absolute amplitude of the wave is plotted versus offset in figures 4.6 and 4.7. All of the reflected arrival curves display cusps which are artifacts of plotting the absolute value. These cusps are due to the reflection coefficients at the boundary changing sign.

We have seen how a positive gradient can act to defocus seismic energy from a boundary. Now, we must consider what happens when a negative gradient is considered. Though velocity profiles that smoothly decrease with depth are rare, investigation of this case is useful when the wavefield is moving up towards a boundary in a material with a positive gradient. This is exactly what happens with the PP phase of seismic body waves in the Earth. The second phase is reflected within the earth so that geometrical spreading is decreased discontinuously at the point of reflection. The reflected ray tube focuses and we can observe a $\pi/2$ phase shift due

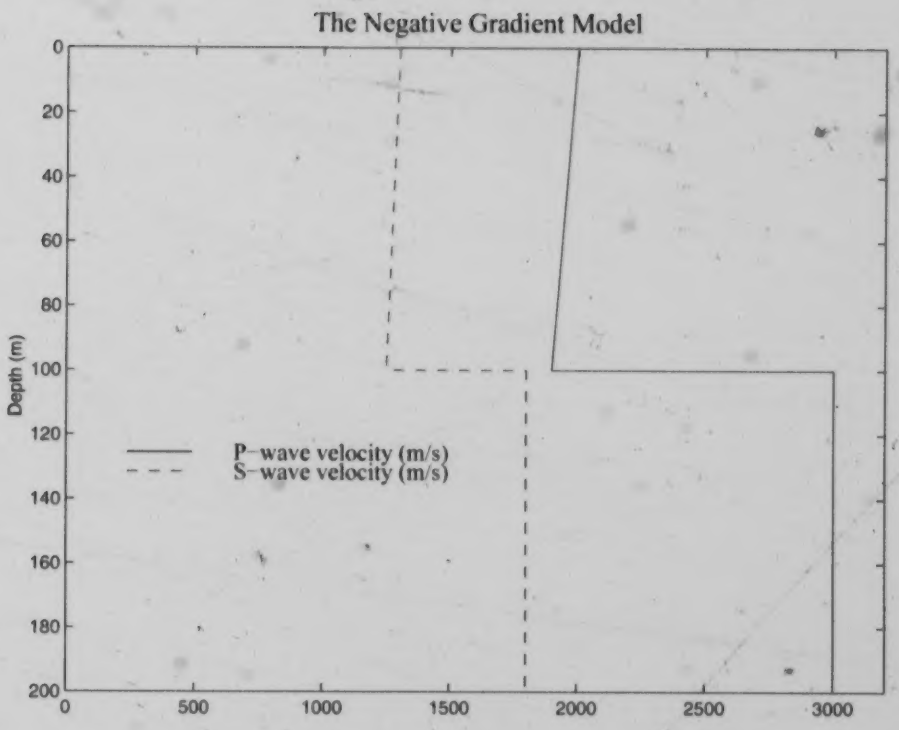

Figure 4.8: The Negative Gradient Model.

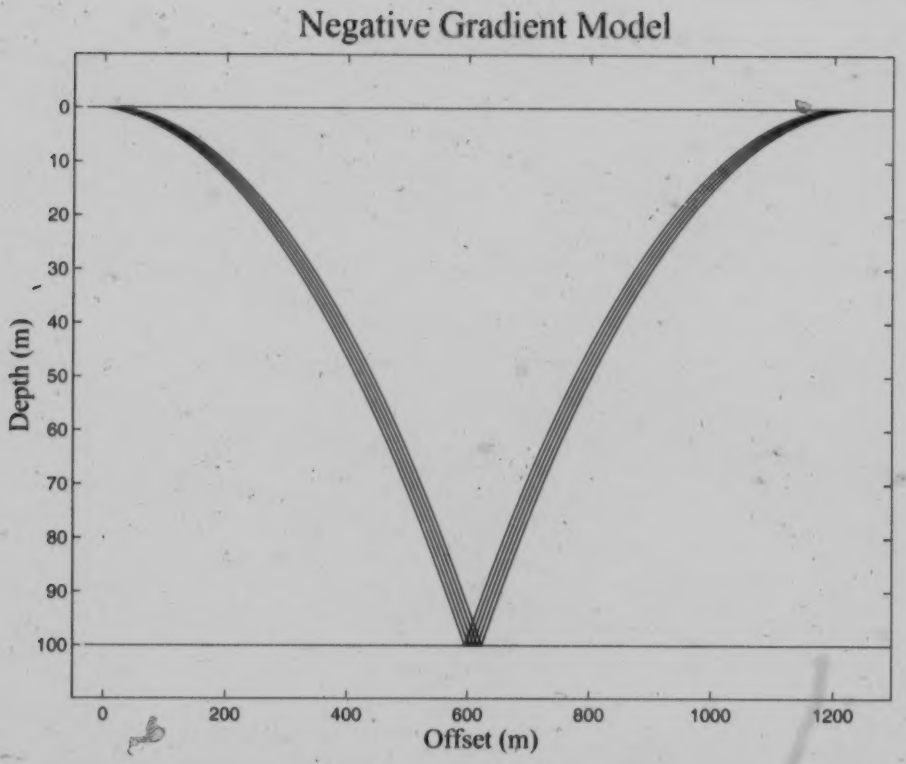

Figure 4.9: Rays for the primary non-phase converted reflection in the Negative Gradient Model.

to the presence of a caustic (Dahlen and Tromp [9]). With that being said, we will consider how seismic energy reflects in a material with a negative gradient. We will introduce the Negative Gradient Model, figure 4.8, which is comprised of a material with a strong negative velocity gradient above a homogeneous layer. The density throughout this model is constant. Figure 4.9 shows the P1P1 arrivals at very high take off angles in this model. The rays appear convex from the surface and it is apparent that some focussing is occurring when the rays return to the surface.

Again, we will consider the primary reflection recorded on the surface from an isotropic point source also located on the surface. The vertical amplitudes for this arrival are plotted in figure 4.10 and the horizontal amplitudes are plotted in figure 4.11. There are large differences observed in the far offset P1P1 cases for both horizontal and vertical components of amplitude. As was observed for the Mississippi Model, the cusps in P1S1 are due to a change of sign in the reflection coefficients. The large horizontal amplitude increase in P1S1 at far offset is not very much due to focussing effects as there exists little difference between the 3rd term excluded curve and the 3rd term included curve. Further inspection revealed that surface conversion coefficients were responsible for this increase (surface conversion coefficients account for the fact the at a free surface, the recorded amplitude consists of reflected waves as well as the incident ray).

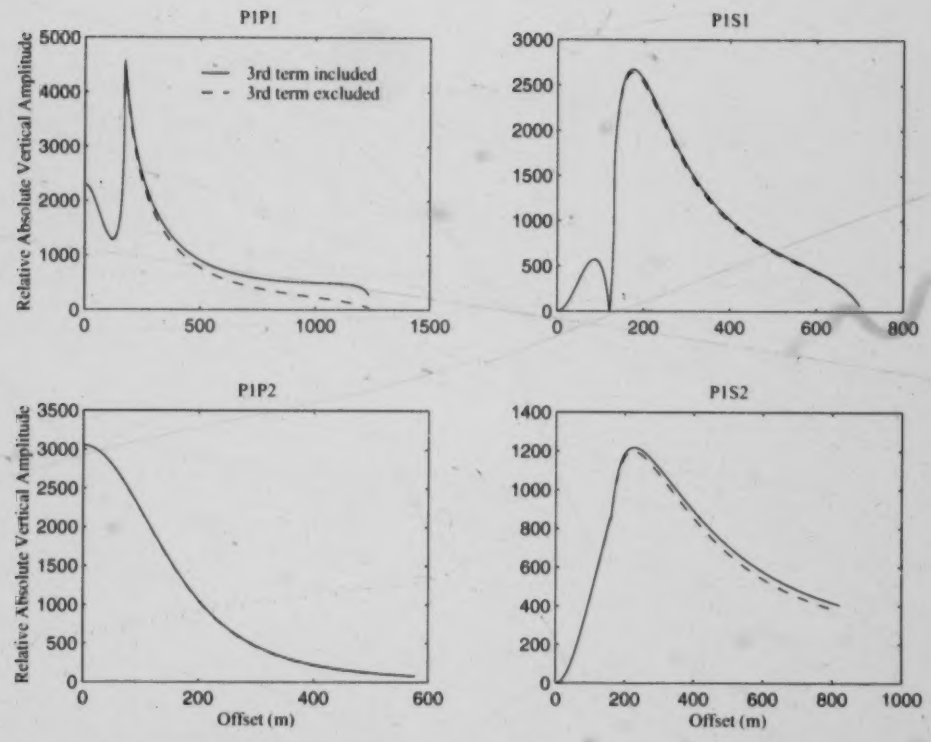

Figure 4.10: The calculated vertical component amplitudes of reflected and transmitted arrivals from an isotropic point source located on the surface of the Negative Gradient Model recorded at a receiver on the surface. The difference in amplitude of the two curves is due to inclusion or exclusion of the effects of velocity gradients on the jump in geometrical spreading across the boundary at 100 m.

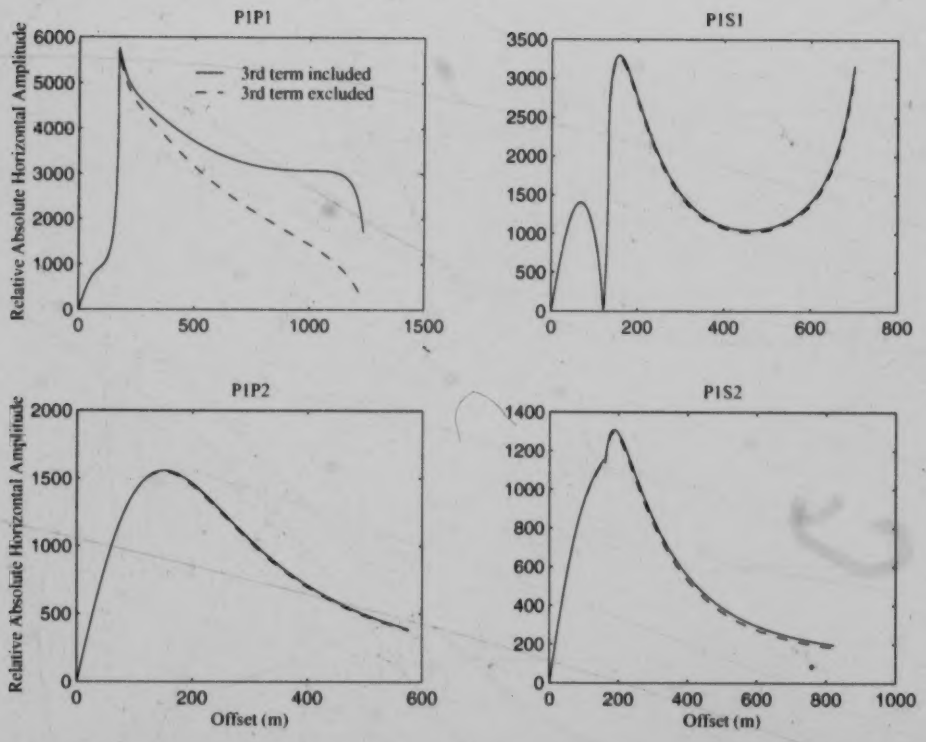

Figure 4.11: The calculated horizontal component amplitudes of reflected and transmitted arrivals from an isotropic point source located on the surface of the Negative Gradient Model recorded at a receiver on the surface. The difference in amplitude of the two curves is due to inclusion or exclusion of the effects of velocity gradients on the jump in geometrical spreading across the boundary at 100 m.

4.3.2 Comparison of Analytical Calculations with the Ray Shooting Method to Determine Geometrical Spreading

We have presented various amplitude versus offset curves for various models but we have not verified our results against an independent method. However, knowing the ray paths of the waves, we can approximately evaluate the geometrical spreading term, L, through the ray shooting method. This method involves shooting two adjacent rays to estimate a derivative in a formula for geometrical spreading. For a medium which is only varying vertically, the geometrical spreading at any point specified by horizontal distance, x, and take off angle, θ_o, is given as

$$L = \sqrt{\frac{x\cos\theta}{\sin\theta_o}\left|\frac{dx}{d\theta_o}\right|} \approx \sqrt{\frac{x\cos\theta}{\sin\theta_o}\left|\frac{\Delta x}{\Delta\theta_o}\right|} \tag{4.26}$$

where θ is the angle between the ray's tangent vector and vertical. In practice, the derivative term, $\frac{dx}{d\theta_o}$, needs to be numerically evaluated so that the resulting value of L is only approximate. Though the equations for this method are presented in Lay and Wallace [24] and Aki and Richards [1] for a spherically symmetric Earth, by taking the limit as the radius of the Earth goes to infinity, we arrive at equation 4.26 valid on flat models. At the surface, for the primary P reflection recorded at the horizontal surface, $\theta = \theta_o$ and $\frac{\Delta x}{\Delta\theta_o}$ can be determined easily by simply shooting rays. Two rays are shot separated by an incremental takeoff angle, $\Delta\theta_o$, and are observed at the surface separated by a distance, Δx.

Figure 4.12 shows the ratio of analytic geometrical spreading (i.e. L calculated using the techniques of the previous section) with the geometrical spreading calculated using the ray shooting method for a wave which is reflected from the

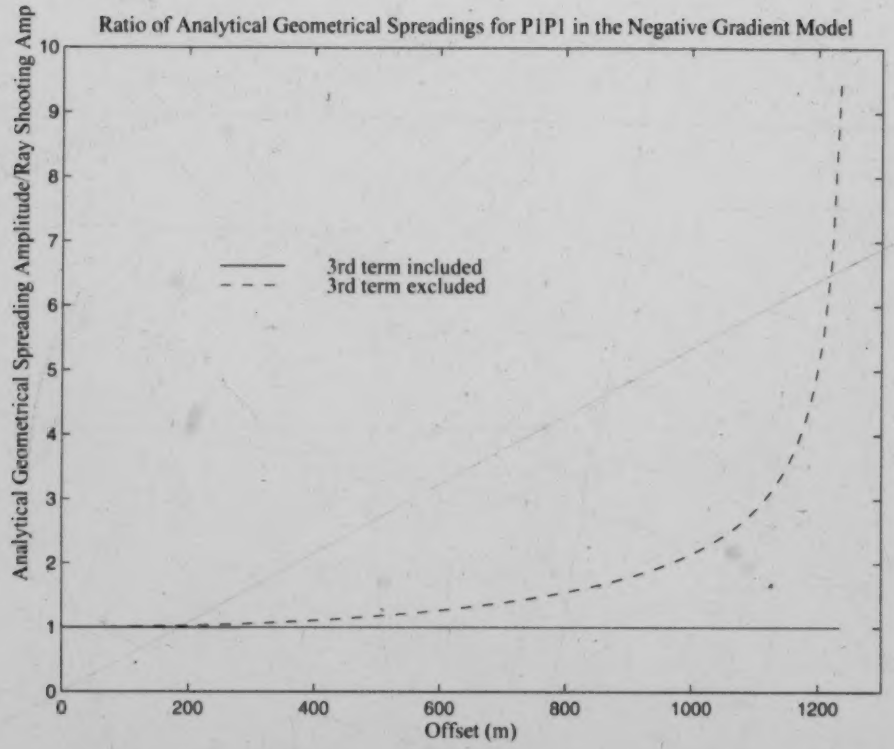

Figure 4.12: A comparison of different calculations of geometrical spreading in the Negative Gradient Model for the P1P1 arrival as recorded at the surface. The two curves represent the numerator of the ratio being equal to the analytic geometrical spreading evaluated by either including or excluding the 3rd term in equation 3.24.

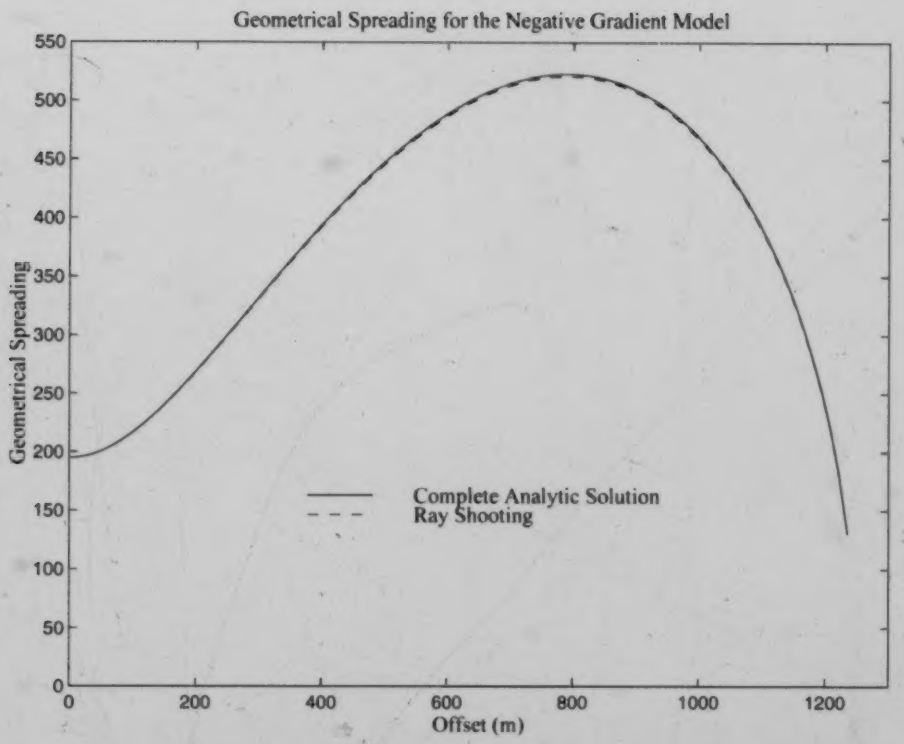

Figure 4.13: A comparison of the complete analytical geometrical spreading with the ray-shooting geometrical spreading in the Negative Gradient Model for the P1P1 arrival as recorded at the surface.

boundary and arrives at the surface. As in previous figures, we have displayed two curves: one curve represents the complete solution as determined by using the 3rd term in equation 3.24; the other curve represents a calculation made by excluding this term. We see that the complete solution is very nearly equal to the approximate (ray-shooting) solution over all values of offset whereas the incomplete (3rd term excluded) solution diverges rapidly until it is almost ten times greater than the ray-shooting solution at the farthest offset. Figure 4.13 shows exactly how little difference there is between the complete solution and the independent approximate solution derived using the ray shooting method. Whatever difference that exists resides with the fact that the ray shooting method is an approximation.

Figure 4.13 also demonstrates interesting properties of how the wave behaves when reflected into a medium with a negative velocity gradient. The geometrical spreading term increases only to a point. This point corresponds to where the wavefront, in the plane of incidence, changes concavity due to the discontinuity in geometrical spreading at the boundary. The geometrical spreading decreases rapidly until the last ray, which in the figures above corresponds to a take off angle of 89.8°, is shot. Further investigation of the ray at a take off angle of 89.9999° revealed that the geometrical spreading of the ray as it returned to the surface had a value of ~ 2.95. We also know that for a negative gradient, the primary reflection has a shadow zone whose edge on the surface may be calculated by evaluating the offset of a ray whose take off angle is 90°. It would appear that this edge represents a caustic in the ray. Thus, we can show that the $\pi/2$ phase shift observed in the PP and SS reflection for a seismic body wave is due to a caustic [9] which, in turn, is due to the velocity gradients at the bounce point causing a change in concavity of the wavefront in the plane of incidence.

CHAPTER 5

Reflections from a Second Order Discontinuity

5.1 Introduction

It was noted by Červený and Ravindra [6] in their discussions of seismic boundary conditions in the Asymptotic Ray Theory approximation that a discrete change in the nth derivative of a material properties also causes a reflection to appear in the nth order term of ART. Most boundaries in a seismological sense are assumed to represent a discrete change in material properties. But, any material which encounters gradual changes in composition or phase after a certain depth should contain discrete discontinuities in the derivatives of these material properties. Such gradational boundaries are believed to be present in the transition zone of the mantle, most notably at the 410 km and 660 km discontinuities and between them. These types of weak boundaries feature two changes in gradient where the central region is where a phase transition or a gradual change in chemical composition is taking place as well as the pressure and temperature effects which exist independently of the former processes. Investigations into these types of transitions, conducted by Gupta [15] and Richards [29], consider the gradational boundary being responsible for one reflection. Gupta obtained theoretical relations for the effect of a transition layer on the observed amplitude and Richards used these relations to constrain the width of the 660 km discontinuity by examining the precursors to the PP arrival. Benz and Vidale [4] later conducted similar studies of PP precursors.

In contrast, ART predicts that a wave whose wavelenth is appreciably less than the extent of the phase transition zone should have two primary reflections, one for each change in gradient. Though current estimates of the thickness of these transition zones are less than a typical seismic wavelength for an earthquake source, these types of transitions can exist in thick sedimentary sequences as well, particularly with materials whose properties are very dependent on the pressure and temperature conditions, such as certain clays. Also, as presented by Wysession et al. [34], some models of the D" discontinuity at the base of the mantle contain changes in seismic velocity gradient with depth. As reflected energy from these types of boundaries scales inversely with frequency relative to the zeroth order amplitude term, such arrivals are likely obscured and difficult to detect. However, scattering of wave energy at discontinuities in velocity gradient should exist and their variations with angle of incidence should be understood.

5.2 Boundary Conditions

For a second order boundary (i.e. a change in gradient), there will exist reflected and transmitted terms in the first order approximation of ART. The first order reflection and transmission coefficient may be analytically determined as, for the $k = 1$ case in equations 2.84 to 2.89, all of the F_i terms ($i = 1, 2, \ldots, 6$) may be determined provided we use a simple model. For an isotropic explosive point source in a homogeneous medium, the wavefield is exactly described by the first order expansion of ART (Vavryčuk and Yamogida [32]) where the amplitude terms for P-waves have the expressions:

$$\vec{W}_o^o = \frac{A}{r}\hat{t} \text{ and} \tag{5.1}$$

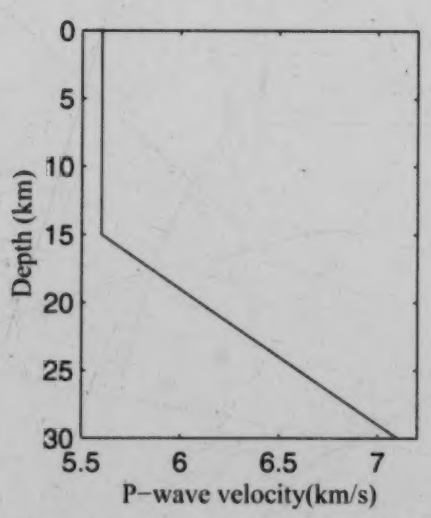

Figure 5.1: The Červený Model.

$$\vec{W}_1^o = \frac{v_p A}{r^2} \hat{t} \tag{5.2}$$

where r is the distance travelled along the ray. Because these terms are well known, we will use a simple model, here called the Červený model, first used by Červený and Zahradník [7] in investigating caustics. This model consists of a homogeneous layer over a lower layer with a constant velocity gradient. This model is shown in figure 5.1. The P-wave velocity is given as a function of depth only and the material is a perfectly elastic Poisson solid ($v_p = \sqrt{3} v_s$) with a constant density.

As the amplitude of the zeroth order term is continuous though the boundary, no zeroth order reflected or transmitted waves in the zeroth order approximation will exist. However, a ray with a non-zero angle of incidence will begin to bend according to the gradient past the boundary. Focussing and defocussing of this zeroth

order term, due to the change in gradient, must also be accounted for as it is required that an exact analytical formula exists for this term. Recalling equations 3.24, 4.19, and 4.21 we have

$$\vec{W}_o^{*3} = \frac{A}{r^*}\hat{t} \tag{5.3}$$

where

$$r^* = r_o\left[\frac{(r'+\Delta r)(r_o+\Delta r)}{r' r_o}\right]^{\frac{1}{2}}, \tag{5.4}$$

$$r' = \frac{r_o v_p \cos\theta}{v_p\cos\theta - g_p r_o \sin^2\theta}, \tag{5.5}$$

$$\Delta r = \frac{v_p + g_p(z-z_o)}{g_p}\sinh(g_p\Delta\tau), \tag{5.6}$$

$$\tag{5.7}$$

z is the depth coordinate ($z = z_o$ at the boundary), g_p is the projection of $\vec{\nabla} v_p$ on the z-axis (we can similarly define g_s as the z-axis projection of $\vec{\nabla} v_s$), θ is the angle of incidence, and $\Delta\tau$ is the traveltime from the boundary, and r_o is the distance from the source to the boundary.

Explicit knowledge of the zeroth order amplitudes is necessary as we need to differentiate these terms to account for the stresses on both sides of the boundary. For the first order stresses associated with the incident wave knowledge of the following derivatives are necessary:

$$\frac{\partial \vec{W}_o^o}{\partial x} = -\frac{A}{r^2}\sin\theta\hat{t} \text{ and} \tag{5.8}$$

$$\frac{\partial \vec{W}_o^o}{\partial z} = -\frac{A}{r^2}\cos\theta\hat{t}. \tag{5.9}$$

For the first order stress terms due to the presence of a zeroth order transmitted wave, we can calculate

$$\left.\frac{\partial \vec{W}_o^{*3}}{\partial \tau}\right|_{\Delta\tau=0} = -\frac{A}{2r_o^2}\left(\frac{2v_p\cos\theta - g_p r_o \sin^2\theta}{\cos\theta}\right)\hat{t} + \frac{Ag_p}{r_o}\sin\theta\hat{n} \tag{5.10}$$

and using

$$\frac{\partial \vec{W}_o^{*3}}{\partial x} = \frac{\partial \vec{W}_o^{*3}}{\partial \tau}\cdot\hat{x}\frac{\hat{x}}{v_p} \text{ and} \tag{5.11}$$

$$\frac{\partial \vec{W}_o^{*3}}{\partial z} = \frac{\partial \vec{W}_o^{*3}}{\partial \tau}\cdot\hat{z}\frac{\hat{z}}{v_p} \tag{5.12}$$

we may determine the necessary partial derivatives.

From the zeroth order term, we may also determine the first order principle component of the associated ray. Vavryčuk and Yamogida [32] determined that for an isotropic point source in a homogeneous medium, there are no principle components. This result applies to the upper medium. Below the boundary, we need to modify equation 2.37 in order to obtain the solution. Noting that the perpendicular projection of $\vec{M}$ may be written as:

$$\vec{M}(\vec{W}_o^{*(3)})\cdot\epsilon_\perp = (\lambda+\mu)\vec{\nabla}\left(\frac{W_{oP}^{*(3)}}{v_p}\right)\cdot\epsilon_\perp + \frac{W_{oP}^{*(3)}}{v_p}\vec{\nabla}\lambda\cdot\epsilon_\perp + 2\mu W_{oP}^{*(3)}\vec{\nabla}\left(\frac{1}{v_p}\right)\cdot\epsilon_\perp \tag{5.13}$$

we can determine the value of the additional component of $\vec{W}_{1P}^{*(3)}$ through equation 2.37. With this method, we obtain:

$$W_{1SV}^{*(3)} = W_{oP}^{*(3)} g_p \sin\theta + \frac{4g_s v_p v_s}{(v_s^2 - v_p^2)} W_{oP}^{*(3)}\sin\theta \text{ and} \tag{5.14}$$

$$W_{1SH}^{*(3)} = 0. \tag{5.15}$$

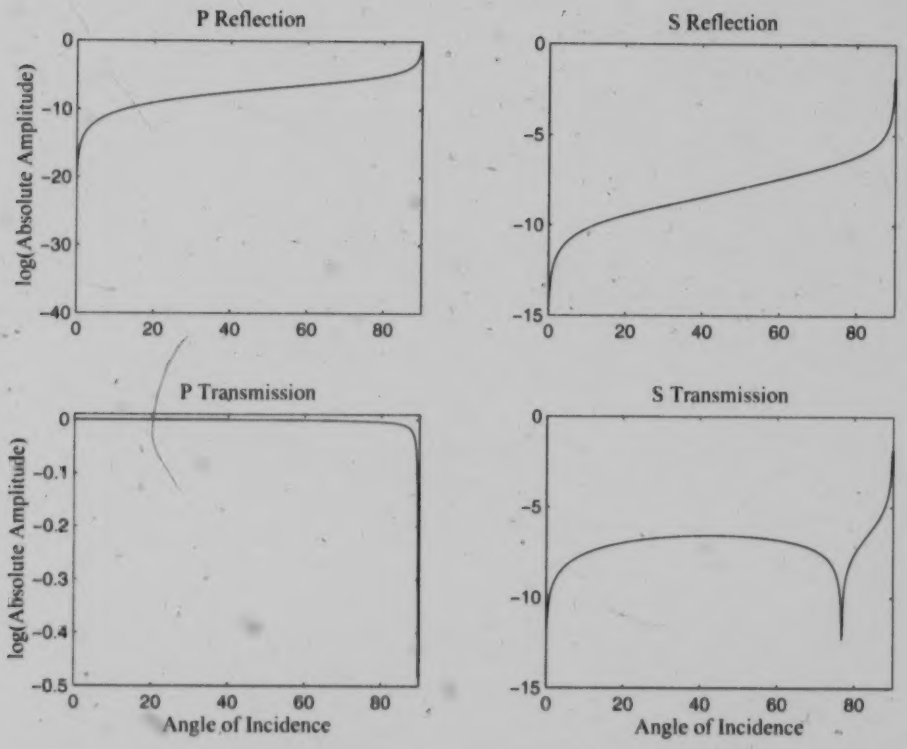

Figure 5.2: Amplitude versus angle curves for first order reflections from the second order discontinuity in the Červený model where $r_o = 150$m.

5.3 First Order Reflected and Transmitted Waves

We have all the formulae necessary to calculate the first order amplitudes of all reflected and transmitted waves at the boundary. Using the Červený model, figure 5.1, we may calculate the amplitudes of all of the reflected and transmitted phases at the boundary. These curves are plotted in figure 5.2 where the source is explosive and it is moved in such a way as to keep the distance from the source to the point of incidence constant (i.e. r_o is constant).

In figure 5.2, we see that at zero incidence all of the first order energy is transmitted and the boundary is transparent. However, as the angle of incidence is increased, more energy is transferred to the first order P and S reflections and the S transmission. These curves do not vanish at high angles of incidence either. This is due to a term in the derivative of the zeroth order transmitted wave (i.e. the leading order term in the ray series) being proportional to $\frac{\sin^2\theta}{\cos\theta}$. However, the effects are very small compared with the zeroth order terms especially since the first order terms are proportional to the inverse of frequency. The first order terms may be differentiated from the other terms as they are accompanied by a $\pi/2$ phase shift. This phase shift, at far offsets, might result in these terms being interpreted as zeroth order diving waves that have passed through a caustic in the lower half of the model.

Another interesting feature of the gradient terms in the derivative is that they, along with the additional component terms, are proportional to $\frac{1}{r_o}$ as opposed to $\frac{1}{r_o^2}$ as are every other term in the boundary conditions. A consequence of this dependence is that the reflection and transmission coefficients depend on the distance from the source to the point of incidence. We may calculate the reflection and transmission coefficients for differing values of r_o in the Červený model to examine this effect. Figures 5.3 and 5.4 show that the reflection and transmission coefficients for $r_o = 1500$m and $r_o = 15000$m have differing values for varying angles of incidence though the shape of the curves are similar.

It is apparent that there is a dependence on scale for the reflected amplitudes shown in Figures 5.2 to 5.3. This dependence may be examined more closely by plotting the first order reflection/transmission coefficients against the distance

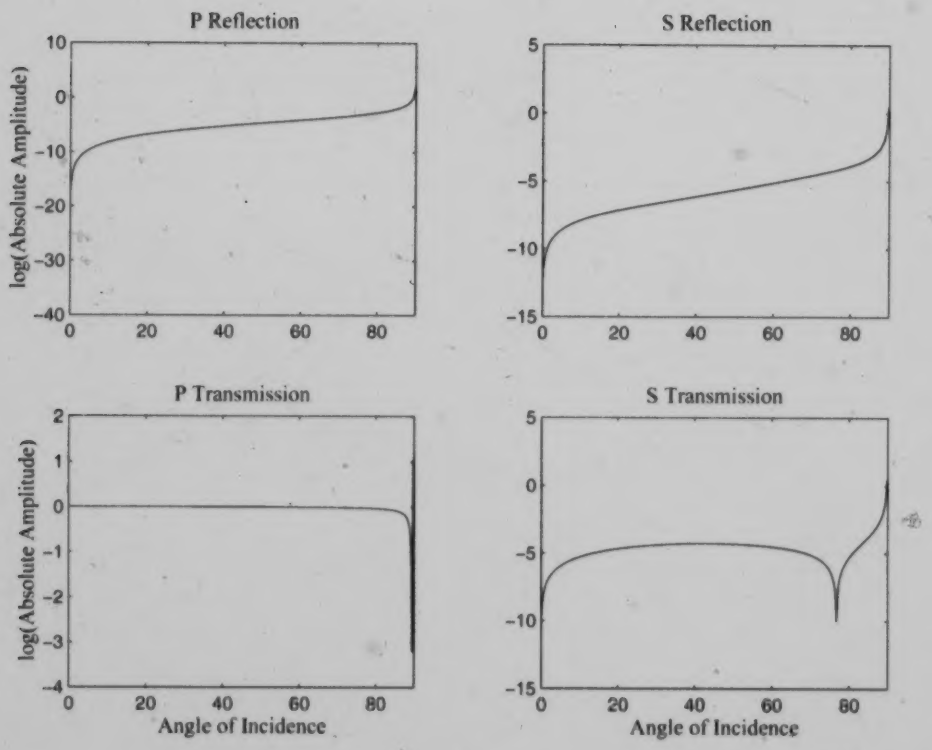

Figure 5.3: Amplitude versus angle curves for first order reflections from the second order discontinuity in the Červený model where $r_o = 1500$m.

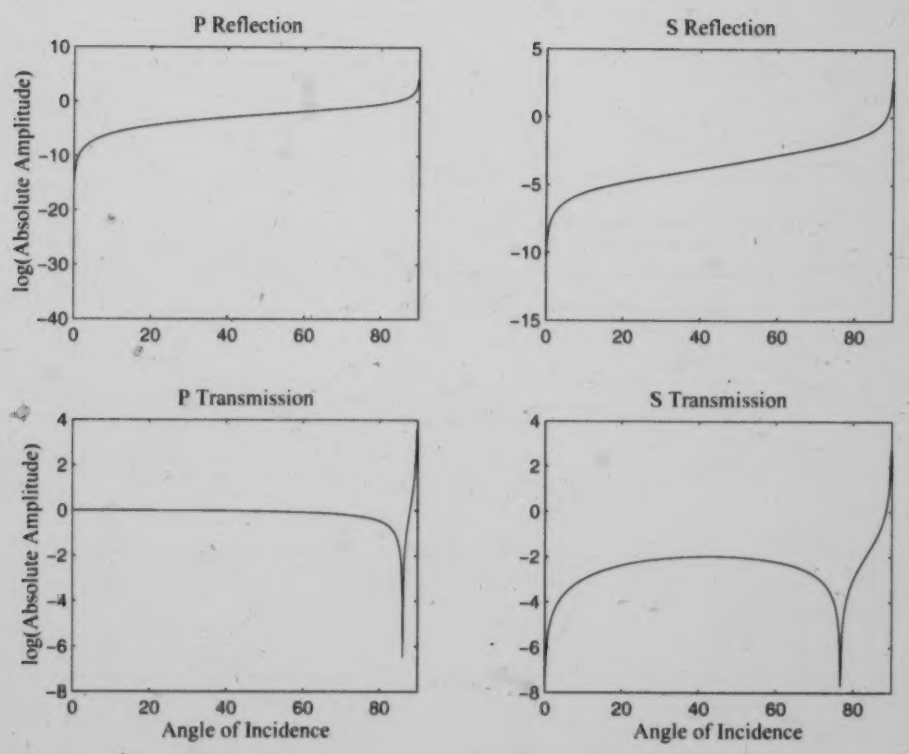

Figure 5.4: Amplitude versus angle curves for first order reflections from the second order discontinuity in the Červený model where $r_o = 15000$m.

to the source from the point of incidence, r_o. The coefficient is simply given as the first order reflected or transmitted amplitude over the first order amplitude of the incident wave. Figure 5.5 is an example of such a plot keeping the angle of incidence constant at 45°. These curves show a linear variation with increasing r_o. This feature arises through the term in the boundary conditions related to the spatial derivatives of zeroth order transmitted P-wave. As shown in equation 5.10 there are terms proportional to $\frac{1}{r_o}$ in this derivative but in all of the other terms in the boundary conditions, the dependence on r_o is inverse square. Therefore, r_o cannot simply be divided out of the boundary conditions and we are left with terms varying linearly with this quantity. Another important note to make is that though reflection and phase converted transmission coefficients diverge linearly from zero at small source to point of incidence distances, the amplitude of the rays actually decrease with r_o as the incident amplitude is proportional to $\frac{1}{r_o^2}$. Therefore, amplitudes are bounded with increasing scale as is physically reasonable.

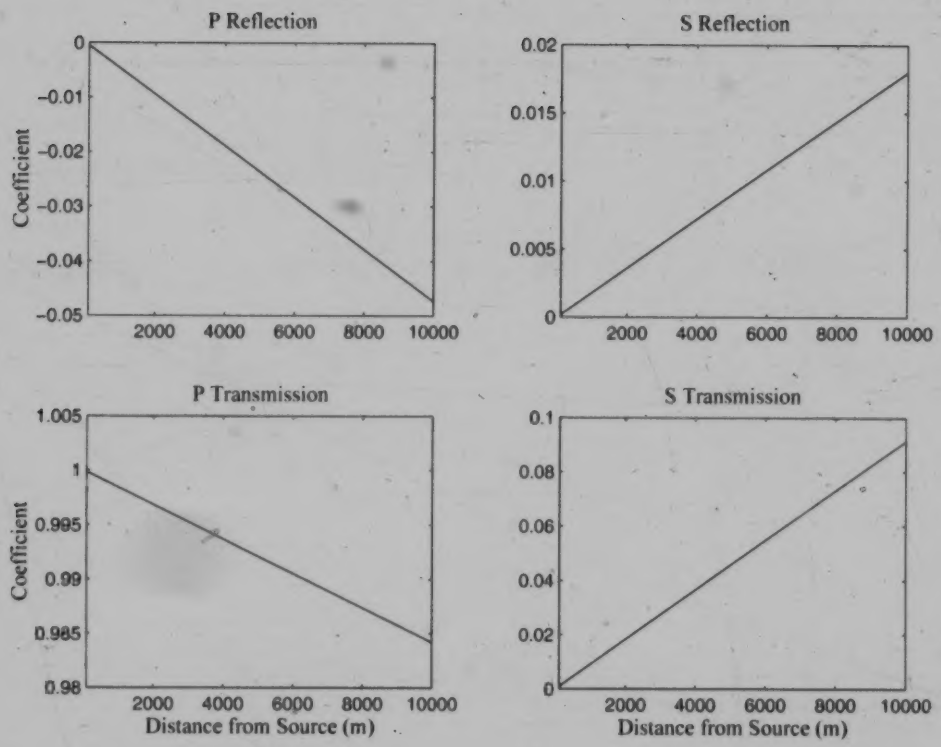

Figure 5.5: Reflection/transmission coefficient versus r_o for the Červený Model. The angle of incidence is 45°.

CHAPTER 6

Conclusions

We have shown that seismic velocity gradients induce effects on the forward modelling of seismic data that do not occur when the models in question only contain constant velocity layers. As velocity gradients occur naturally in most geological layers, it is important to know how they will affect observed seismic data. Specifically, a change in velocity gradient causes energy partitioning at this weak interface as described in chapter 5. This partitioning relies on the focussing and defocussing effects described in chapter 4 as the nature of the leading order ART term away from the boundary influences the boundary conditions as described in chapter 2. The focussing and defocussing effects are a consequence of the dynamic ray tracing system applied over a boundary which was developed in chapter 3 to determine the amplitudes of the leading term in the ray series. Gel'chinskiy's equations also describe these focussing effects and they were proven to be equivalent to the system developed in this chapter.

The techniques described in this thesis to evaluate seismic amplitudes follow a ray approach to modelling as opposed to a full wavefield approach. The difference in these two techniques is that, in general, the former is computationally faster as no cumbersome integrals need to be evaluated over all space as is the case in the latter method. However, ray methods are only valid as high frequency approximations and though they can yield analytical formulae for the wavefield, a

full wave solution is valid over all frequencies and gives a more accurate solution. ART has an advantage over the traditional geometrical ray theory in that some interesting effects of the wavefield (i.e. head waves or reflections from a change in gradient as described in this thesis) can be detected by only going through the effort of evaluating the first two terms in the ray series. Though more accuracy may be obtained initially by evaluating more terms, it is important to realize that the ray series is asymptotically convergent and after a certain number of terms, the series will begin to diverge. Thus, it is not desirable to evaluate an infinite number of terms.

Bibliography

[1] K. Aki and P. G. Richards. *Quantitative Seismology Theory and Methods.* W. H. Freeman and Company, 1980.

[2] V. M. Babich and A. S. Alekseev. A ray method of computing wave front intensities. *Izvestiya, Academy of Sciences, USSR, Geophysics Series*, 1:9–15, 1958. (in Russian).

[3] V. M. Babich and A. P. Kiselev. Non-geometrical waves — are there any? An asymptotic description of some 'non-geomtrical' phenomena in seismic wave propagation. *Geophys. J. Int.*, 99:415–420, 1989.

[4] H. M. Benz and J. E. Vidale. The sharpness of upper mantle discontinuities determined from high frequency P'P' precursors. *Nature*, 365:147–150, 1993.

[5] V. Červený and F. Hron. The ray series method and dynamic ray tracing system for three-dimensional inhomogeneous media. *Bull. Seism. Soc. Am.*, 70:44–77, 1980.

[6] V. Červený and R. Ravindra. *Theory of Seismic Head Waves.* University of Toronto Press, 1971.

[7] V. Červený and J. Zahradník. Amplitude-distance curves of seismic body waves in the neighbourhood of critical points and caustics — a comparison. *Z. Geophys.*, 38:499–516, 1972.

[8] A. Choi. Rays and caustics in vertically inhomogeneous elastic media. Master's thesis, University of Alberta, 1978.

[9] F. A. Dahlen and J. Tromp. *Theoretical Global Seismology.* Princeton University Press, 1998.

[10] G. A. Deschamps. Ray techniques in electromagnetics. *Proc. IEEE*, 60:1022–1035, 1972.

[11] M. P. do Carmo. *Differential Geometry of Curves and Surfaces.* Prentice-Hall Inc., 1976.

[12] A. M. Dziewonski and D. L. Anderson. Preliminary reference Earth model. *Phys. Earth Planet. Inter.*, 25:297–356, 1981.

[13] C. M. R. Fowler. *The Solid Earth An Introduction to Global Geophysics.* Cambridge University Press, 1990.

[14] B. Y. Gel'chinsky. Expression for the spreading function. *Problems in the Dynamic Theory of Seismic Wave Propagation*, 5:47–53, 1961. (in Russian).

[15] R. N. Gupta. Reflection of elastic waves from a linear transition layer. *Bull. Seism. Soc. Am.*, 56:511–526, 1966.

[16] F. Hron. Introduction to A.R.T. in seismology. Geophysics 624 class notes, University of Alberta, 1984.

[17] F. Hron and E. R. Kanasewich. Synthetic seismograms for deep sounding studies using asymptotic ray theory. *Bull. Seism. Soc. Am.*, 61:1169–1200, 1971.

[18] F. Hron and B. G. Mikhailenko. Numerical modeling of nongeometrical effects by the Alekseev-Mikhailenko method. *Bull. Seism. Soc. Am.*, 71:1011–1029, 1981.

[19] F. Hron and B. S. Zheng. On the longitudinal component of the particle motion carried by the shear *PS* wave reflected from the free surface at normal incidence. *Bull. Seism. Soc. Am.*, 83:1610–1616, 1993.

[20] P. Hubral. Wavefront curvature in three-dimensionally laterally inhomogenous media with curved interfaces. *Geophys.*, 45:905–913, 1980.

[21] G. L. James. *Geometrical Theory of Diffraction for Electromagnetic Waves.* P. Peregrinus Ltd., 1976.

[22] F. C. Karal and J. B. Keller. Elastic wave propagation in homogeneous and inhomogeneous media. *J. Acoust. Soc. Am.*, 31:694–705, 1959.

[23] E. S. Krebes and F. Hron. Ray-synthetic seismograms for *SH* waves in anelastic media. *Bull. Seism. Soc. Am.*, 70:29–46, 1980.

[24] T. Lay and T. C. Wallace. *Modern Global Seismology.* Academic Press, 1995.

[25] S. W. Lee. Electromagnetic reflection from a conducting surface: geometrical optics solution. *IEEE trans.*, AP-23:184–191, 1975.

[26] L. W. Marks. *Computational topics in ray seismology.* PhD thesis, University of Alberta, 1980.

[27] T. G. Masters and P. M. Shearer. Seismic models of the earth: Elastic and anelastic. In T. J. Ahrens, editor, *Global Earth Physics A Handbook of Physical Constants AGU Reference Shelf 1*, pages 88–103. American Geophysical Union, 1995.

[28] L. Nettleton. *Geophysical Prospecting for Oil.* McGraw-Hill, 1940.

[29] P. Richards. Seismic waves reflected from velocity gradient anomalies within the earth's upper mantle. *Z. Geophys.*, 38:517–527, 1972.

[30] W. M. Telford, L. P. Geldart, and R. E. Sheriff. *Applied Geophysics.* Cambridge University Press, second edition, 1990.

[31] V. Vavryčuk. Elastodynamc and elastostatic Green tensors for homogeneous weak transversely isotropic media. *Geophys. J. Int*, 130:786–800, 1997.

[32] V. Vavryčuk and K. Yomogida. Multipolar elastic fields in homogeneous isotropic media by higher-order ray approximations. *Geophys. J. Int.*, 121:925–932, 1995.

[33] V. Vavryčuk and K. Yomogida. SH-wave Green tensor for homogeneous transversely isotropic media by higher-order approximation in asymptotic ray theory. *Wave Motion*, 23:83–93, 1996.

[34] M. E. Wysession, T. L. Shearer, J. Revenaugh, Q. Williams, E. J. Garnero, R. Jeanloz, and L. H. Kellogg. The D" discontinuity and its implications. In M. Gurnis, M. E. Wysession, E. Knittle, and B. A. Buffett, editors, *The Core-Mantle Boundary Region*, pages 273–298. American Geophysical Union, 1998.